

Accepted Manuscript

Exploration of chromen-4-one based scaffold's potential in Alzheimer's disease: Design, Synthesis and Biological evaluations

Manjinder Singh, Maninder Kaur, Nirmal Singh, Om Silakari

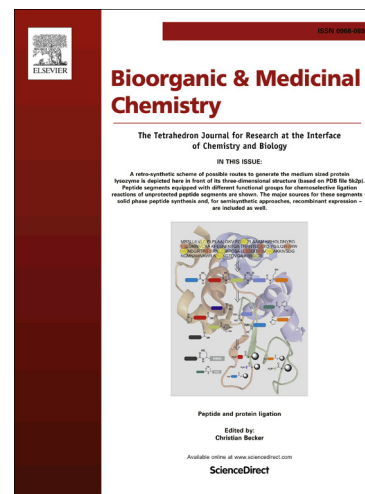
PII: S0968-0896(17)30935-5
DOI: <http://dx.doi.org/10.1016/j.bmc.2017.09.012>
Reference: BMC 13972

To appear in: *Bioorganic & Medicinal Chemistry*

Received Date: 4 May 2017
Revised Date: 1 September 2017
Accepted Date: 9 September 2017

Please cite this article as: Singh, M., Kaur, M., Singh, N., Silakari, O., Exploration of chromen-4-one based scaffold's potential in Alzheimer's disease: Design, Synthesis and Biological evaluations, *Bioorganic & Medicinal Chemistry* (2017), doi: <http://dx.doi.org/10.1016/j.bmc.2017.09.012>

This is a PDF file of an unedited manuscript that has been accepted for publication. As a service to our customers we are providing this early version of the manuscript. The manuscript will undergo copyediting, typesetting, and review of the resulting proof before it is published in its final form. Please note that during the production process errors may be discovered which could affect the content, and all legal disclaimers that apply to the journal pertain.



**Exploration of chromen-4-one based scaffold's potential in
Alzheimer's disease: Design, Synthesis and Biological evaluations**

Manjinder Singh^a, Maninder Kaur^a, Nirmal Singh^a, Om Silakari^{a,*}

*^aDepartment of Pharmaceutical Sciences and Drug Research, Punjabi university, Patiala,
Punjab, India, 147002.*

**E-mail: omsilakari@gmail.com, Telephone: +919501542696*

ABSTRACT

A novel series of flavonoid based compounds were designed, synthesized and biologically evaluated for Acetylcholinesterase (AChE) inhibitory activity integrated with advanced glycation end products (AGEs) inhibitory and antioxidant potential. Most of the derivatives inhibited AChE in nanomolar IC_{50} range along with good AGEs inhibitory and radical scavenging activity. Among them, **7m**, strongly inhibited AChE ($IC_{50}=5.87$ nM) and found to be potent as compared to the reference drug donepezil ($IC_{50}=12.7$ nM). Its potent inhibitory activity has been justified by docking analysis that revealed its dual binding characteristic with both CAS (catalytic active site) and PAS (peripheral anionic site) of AChE, simultaneously. Additionally, this compound also displayed ability to prevent advanced glycation end products formation ($IC_{50}=23.0$ μ M) with additional radical scavenging property ($IC_{50}=37.12$ nM). It (**7m**) also ameliorated scopolamine induced memory deficit in mice employing Morris water maze test. Thus, flavonoids might be the promising lead compounds as potential polyfunctional anti-Alzheimer's agents.

Keywords: Alzheimer's disease, Acetylcholinesterase, Antioxidants, Flavonoids, AGEs, Morris water maze

1. Introduction

Alzheimer's disease (AD) is a complex neurodegenerative disorder among elderly people characterized with gradual decline in various cognitive, executive and memory functions.¹ Other than A β (β -amyloid) deposits, τ -protein aggregation and low ACh level, oxidative damage is eminently observed in AD brains.² In cholinergic hypothesis, the acetylcholine, a neurotransmitter responsible for behavior, memory, cognitive functions and emotions in the brain areas is reduced because of its prompt hydrolysis by AChE enzyme. Additionally, it also promotes the amyloid- β deposition, which further develop the senile plaques.³ Acetylcholinesterase inhibitors (AChEIs) could upsurge the ACh level through AChE inhibition in patients of AD and, therefore, relieve some symptoms experienced by patients. Till date, cholinergic hypothesis based therapeutic approach with AChEIs such as rivastigmine, donepezil and galantamine has been used clinically for AD management.⁴ Therefore, inhibition of AChE has been considered for the management of AD as it may increase acetylcholine level and decrease A β deposition in the brain regions.

Furthermore, numerous evidences suggested the degrading influence of oxidative stress in the AD pathophysiology and progression. Present reports specified that the oxidative impairment may possibly endorse the amyloid plaques and neurofibrillary tangles formation in AD.⁵ The increased level of reactive carbonyls and free radicals leads to form the AGEs, the macroproteins, formed via Maillard reaction (non-enzymatic glycation) also complicated the AD pathogenesis. It cross-linked and glycated the A β or tau proteins, cell death of neurons and glial induction. Moreover, it interact with cell surface receptors RAGE (receptor for AGEs) that provokes the generation of superoxide radicals, hydrogen peroxide, vascular inflammation etc., ultimately contribute to AD pathology.⁶ Consequently, drugs that have the capacity to prevent or scavenge the free radicals generation and AGEs inhibitory potential could help for the management of AD.

The complex nature of AD demands the designing of polyfunctional agents which could simultaneously act on more than one pathway rather than only one. It also implemented diverse biological properties with single bioavailability and pharmacokinetic metabolism. In the present study, the well-established molecular pathways *i.e.* AChE, oxidative stress, and AGEs have been explored for the designing of flavonoid based polyfunctional agents for more effective therapy

of AD than existing one. Flavonoid was considered for designing as it possesses a broad pharmacological properties range like anti-inflammatory, anti-oxidative, AGEs inhibitory effects, and neuroprotective effects against AChE.⁷ Thus, the designing and synthesis of new polyfunctional flavonoid derivatives is an interesting strategy for AD management.

The SAR of our previously reported flavonoids based novel AChE inhibitors,⁸ focused our attention to design more flavonoid derivatives bearing a suitable tertiary amino group, which characterizes the crucial requirement for good AChE inhibitory activity, linked with different lengths of alkyl side chain with variedly substituted flavonoid scaffold. Therefore, we here present work involving the synthesis of flavonoid based novel polyfunctional agents, which were primarily evaluated for *in vitro* AChE inhibition, AGEs inhibition, antioxidant effect and molecular modeling studies. Additionally, *in vivo* anti-amnesic and antioxidant activities of the most active polyfunctional agent were determined.

2. Result and Discussion

2.1 Chemistry

Firstly, to evaluate the influence of different number of methoxy groups at ring-B with hydroxyl group at 7th position of ring-A over the biological activities of flavonoids, compounds **5(a-c)**, were synthesized using well established Baker-Venkataraman rearrangement with slight modifications is outlined in **Scheme 1**.⁹

Our research group previously reported various flavonoids having methoxy group on ring-B and substituted cyclic amine on ring-A via two carbon spacer. Based on those observations, the hydroxyl group of **5(a-c)**, was replaced by 4-methylpiperidine and 4-hydroxyethyl piperazine amines linked via different carbon spacers of 4'-methoxy substituted flavonoids. The synthetic methodologies employed to develop intermediates **6(a-e)** and target compounds **7(a-j)**, are outlined in **scheme 2** and **3**. Firstly, the **5(a-c)** were alkylated with dibromoalkanes in acetone that delivered intermediates **6(a-e)** in satisfactory yields. Finally, the reaction of **6(a-e)** with commercially available secondary amines under reflux in acetonitrile in the presence of K₂CO₃ produced the final compounds **7(a-j)** in 50–80% yields.

Further, synthesis of the compounds **7(k-n)**, with additional methoxy groups at ring-B and 4-methylpiperidinoalkoxy substituent attached at ring- B via two (**7k** and **7m**) and three (**7l** and **7n**) carbon spacer were accomplished using same procedures as shown in **Scheme 3**.

2.2 *In vitro* inhibition studies on AChE

To investigate the potential of synthesized compounds **5(a-c)** and **7(a-n)** for the management of AD, their inhibition towards AChE (brain homogenate) was determined using donepezil as standard compound.¹⁰ The results of all tested derivatives are summarized in **Table 1**. Among the 7-hydroxyl derivatives **5(a-c)**, **5a** with 4'-methoxy at ring-B was found to possess better IC₅₀ value 35.0 nM than compounds **5b** and **5c** (IC₅₀=37.3, 44.2 nM, respectively).

Another series **7(a-j)**, with a methoxy group at the ring-B and different cyclic amines having varied alkyl side chains at ring-A, showed greater AChE inhibitory potential as compared to **5(a-c)**. The alkylation of hydroxyl group at the ring-A in **5(a-c)** with propyl to pentyl carbon chain cyclic amino significantly increased AChE inhibitory potency (**7(a-f)**, IC₅₀ ranges from 7.7 to 17.3 nM) indicating the significance of the quaternary amine than the hydroxyl group. However further increase in carbon spacer reduced the activity by 3-fold (**7(g-j)**, IC₅₀ ranges from 48.1 to 67.2 nM).

As presented in **Table 1**, among all (**7a-7j**), compounds **7a** and **7b** showed most potent inhibitory activity against AChE having IC₅₀ values of 7.7 and 8.2 nM, respectively. The effect of different carbon chain linkers attached to aminoalkyl moiety on AChE inhibition were also studied and observed that on increasing the chain length from four to eight carbons, the activity was reduced (**7(c-j)**, IC₅₀ =13.53-67.2 nM) than compounds having two to three carbon (**7(a-b)** and **7(k-n)**, IC₅₀ =5.87-8.25 nM), thus ethyl to propyl alkyl chain length is optimum of cyclic aminoalkyl groups for AChE inhibition. The substitution with additional -OCH₃ group at ring-B reliably enhanced the AChE inhibition with IC₅₀ values ranges from 5.87-6.77 nM. The 3',4',5'-Trimethoxy substituted compounds (**7m** and **7n**, IC₅₀ = 5.87 and 6.12 nM) showed good potencies than 3',4'-Dimethoxy-substituted derivatives (**7l** and **7k**, IC₅₀ = 6.48 and 6.77 nM).

Overall, the 3',4',5'-Trimethoxy-substituted flavone **7m** was found to be most active compound having IC₅₀ value of 5.87 nM, which is 2-fold of donepezil activity (IC₅₀=12.7 nM). Therefore, compound **7m** was selected for *in vivo* evaluation.

2.3 Advanced glycation end-product formation inhibitory activity

All the synthesized compounds **5(a-c)** and **7(a-n)** were subjected to *in vitro* bioassay of AGEs formation inhibitory activity summarized in Table 1.¹¹ Among the various synthesized compounds, the compound **7m** ($IC_{50}=37.1 \mu M$) was found to be comparable to the reference drug aminoguanidine ($IC_{50}=40.0 \mu M$). The compounds **7d**, **7n**, **7k**, **7a**, **5a** and **7b** (IC_{50} value ranging from 38.4 to 43.1 μM) showed good to moderate inhibitory activity with respect to the reference drug. However, the compounds **5b**, **7l**, **7c**, **7f**, **7h**, **5c**, **7j**, **7e**, **7g** and **7i** (IC_{50} value ranging from 47.4 to 61.1 μM) displayed lower anti-glycating activity than the standard drug. As evident from the results, the derivatives having alkyloxy linked to hydroxyethyl piperazine substitution at 7th position of ring-A and 4'-methoxy ring-B of flavone (**7b**, **7d**, **7f**, **7h** and **7j**) were found to be more active than the derivatives with 4-methylpiperidine alkyloxy at position 7th of ring-A (**7c**, **7e**, **7g** and **7i**). The compound with 4-methylpiperidine moiety at position 7th of ring-A and 3',4',5'-trimethoxy on ring-B of flavone (**7m**) was found to be more active than the compounds with 3',4'-dimethoxy (**7k** and **7l**, $IC_{50}=42.1$, 47.7 μM , respectively) and mono methoxy (**7a**, $IC_{50}=42.6 \mu M$) on ring-B. The most active compound **7m** ($IC_{50}=37.1 \mu M$), 4-methylpiperidine linked using two carbon spacer showed good activity as compared to compound **7n** ($IC_{50}=41.7 \mu M$) having 4-methylpiperidine moiety linked using three carbon spacer. The flavonoid **5a** ($IC_{50}=42.0 \mu M$) having hydroxyl at position 7th of ring-A and 4'-methoxy at ring-B of flavone exhibited good activity than compounds **5b** and **5c** ($IC_{50}=47.4$, 51.4 μM , respectively) having 3',4'-dimethoxy and 3',4',5'-trimethoxy at ring-B of flavone, respectively.

2.4 *In vitro* antioxidant activity

Synthesized compounds **5(a-c)** and **7(a-n)** were evaluated for *in vitro* antioxidant activity¹² and results are showed in **Table 1**. Results noticeably indicate that almost all the compounds displayed radical scavenging activity. Among them, **5a**, **5b**, **7k**, **7b** & **7m** ($EC_{50}=20.5-23.0$ nM) were comparable to ascorbic acid $EC_{50}=20.0$ nM. The compound **5a** was found to be the best radical scavenger ($EC_{50}=20.5$ nM), might be due to the hydroxyl group. The derivatives with 4-(2-hydroxyethyl)piperazine-1-yl)alkoxy substitution at 7th position of ring-A (**7b**, **7d**, **7f** and **7j**, EC_{50} ranges from 22.7-35.7 nM) were found to be more active than the derivatives with 4-

methylpiperidine alkyloxy at same position (**7a**, **7c**, **7e** and **7i**, EC₅₀ ranges from 26.5-42.6 nM). The compounds with 2-(4-methylpiperidin-1-yl)ethoxy substituent showed good activity (**7k** and **7m**, EC₅₀=22.7, 23.0 nM, respectively) as compared to compounds with 3-(4-methylpiperidin-1-yl)propoxy substituent (**7l** and **7n**, EC₅₀=24.1, 26.8 nM, respectively). Furthermore, increase in the chain length *s* of alkyl spacer between ‘O’ and ‘N’ of substituents decrease the radical scavenging activity by 1.5-2.0 fold. The double bond between C₂=C₃ in conjugation with a carbonyl at C₄ of flavonoid moiety provides electron delocalization from the ring-B, appears to be crucial to scavenge the free radicals. Conjugation system of ring-A and B showed extended resonance effect providing increased radical stability to the flavonoid nucleus.¹³

2.5 Kinetic characterization of AChE inhibition

Based on the *in vitro* results of AChE inhibition, the kinetic study was carried out on most potent inhibitor **7m** to determine the kind of enzyme inhibition. The Lineweaver–Burk plots displayed both increased intercepts (higher K_m) and slopes (decreased V_{max}) at higher concentration of compound **7m**, indicating a mixed type of inhibition (**Fig. 1**). Thus, compound **7m** have the ability to bind with both CAS as well as PAS of AChE enzyme.

2.6 Molecular docking studies

In order to discover the interaction patterns of flavonoids with AChE enzyme, docking studies were carried out for the most potent inhibitor **7m** with *Torpedo californica* AChE (TcAChE, 1EVE) crystal structure.^{14,15} Its 3D structure contains an active site situated at deep and narrow gorge bottom comprising of Phe330 and Trp84 amino acid residues in the catalytic anionic site. Additionally, aromatic residues Tyr70, Tyr121, Tyr334, Asp72 and Trp279 of peripheral anionic site located near the gorge of active site.¹⁶ The compound **7m** showed nice fit in active site by binding with both CAS and PAS of the AChE enzyme simultaneously to afford maximal inhibition. The binding pattern of compound **7m** with AChE binding site is shown in **Fig. 2**.

As shown in **Fig. 2**, the compound **7m** binds along the active-site gorge, extending from the anionic subsite near Trp84 to the peripheral anionic site (PAS) near Trp279. The protonated nitrogen atom the 4-methylpiperidine moiety of compound **7m**, displayed cation- π interaction with conserved amino acid residue Trp279, a major component of a peripheral “anionic” site (PAS) which is 14 Å far from the active site and nearby to gorge top of the enzyme. It also

interacts with Ser286 of PAS via hydrogen bonding. Ring-B of flavonoidal scaffold showed π - π stacking with Phe331, in acyl binding pocket. The ring-B also interacts with catalytic triad of CAS, accountable for ACh ester bond hydrolysis, via π - π stacking with His440 amino acid and hydrogen bonding of methoxy group at ring-B with Ser200 amino acid. The 'O' of $-OCH_3$ group also forms H-bond with peptidic amino groups of Gly118, another residue located in the esteric subsite. The docking study of **7m** revealed the dual binding property as it interacted with both catalytic as well as peripheral anionic site via hydrogen bond, π - π (aromatic) and hydrophobic interactions. (**Fig. 2**)

2.7 Molecular Dynamic Simulations

Molecular dynamic simulation (MD) was undertaken to identify the ligand-protein interactions in dynamic motion contributing for thermodynamic stability and to envisage the effect on conformational changes induced by ligand binding at AChE pocket.¹⁷

The protein ligand binding complex of AChE and the most active compound **7m** was used for MD simulations. After MD, although the important interactions were conserved, some additional interactions were also observed. After MD, compound **7m** displayed cation- π interactions with Trp279 amino acid of PAS. It also showed π - π stacking interactions with Trp84 amino acid of CAS and strong hydrogen bonding with Ser81 (**Fig. 3A**). These interactions are summarized in the protein-ligand contacts plot (**Fig. 3B**). After MD simulations, the RMSD (Root mean square deviation) was calculated for trajectory of complex and plotted against time (ns). The plot of RMSD showed, docked complex was quite stable all the way through with minor fluctuations in the range of 1–1.5 Å (**Fig. 3C**). The stability of the simulated system indicates the inhibitory nature of the **7m** on AChE.

2.8 ADMET prediction

To envisage the drug likeness of the synthesized compounds, different indicators of pharmacokinetic profile like Lipinski's parameters, QPlogPo/w, Polar Surface Area (PSA), QPlogKhsa, QPPCaco, QPlogBB, QPLogKhsa, QPlogBB, QPPMDCK etc. were predicted with QikProp module.^{18,19} (**Table 2**)

The important features of drugs acting on CNS should have the ability to cross BBB (blood brain barrier). The results showed that synthesized compounds **5(a-c)** and **7(a-n)** obey Lipinski's

rule of five (mol_MW <500, QPlogPo/w <5, donorHB≤5, acptHB≤10) and therefore are drug like molecules. The results for CNS activity and QPlogBB showed that all synthesized compounds have the ability to enter into the brain. PSA (polar surface area) also predicted the ability to pass through BBB. For a compound to be CNS active, PSA should be lower to penetrate the BBB and the value should be less than 90 Å.²⁰ The QPlogKhsa value determined the protein binding amount of CNS active drugs which is also a vital consideration and be likely to moderately high. The QPlogKhsa values for all compounds **5(a-c)** and **7(a-n)** showed their strong plasma protein binding. All the synthesized compounds are able to cross the BBB though their PSA values are within acceptable limits (56-85 Å). Among predicted parameters, QPlogBB, QPLogKhsa, QPPMDCK and QPPCaco primarily reflect the capability of the compound's distribution in the body. Majority of the compounds exhibited moderate to significant penetrability for *in vitro* MDCK cells as well as *in vitro* Caco-2 cells. The pharmacokinetic parameters prediction disclosed that all synthesized compounds **5(a-c)** and **7(a-n)**, have drug like properties. Further, to estimate relative binding affinity of all the synthesized compounds MM-GBSA binding energies were calculated as showed in **Table 2**. The energy of all the synthesized derivatives ranges from -42.534 to -99.832, comparable to MM-GBSA energy of donepezil -78.70, thus signifying durable ligand-enzyme binding interactions.

2.9 *In vivo* activity on scopolamine induced amnesia in mice assessed on Morris water maze.

The compound **7m** was further assessed for memory restoration in scopolamine induced amnesia in mice.²¹ Administration of scopolamine (0.5 mg/kg) significantly decreased ELT (escape latency time) on day 4 and TSTQ (time spent in target quadrant) on day 5 signifying the memory loss as evaluated using Morris water maze as compared to normal mice. Administration with donepezil (2 mg/kg) significantly reversed amnesia induced by scopolamine in comparison with scopolamine treated animals. Similarly, treatment with **7m** (2, 5 and 10 mg/kg) significantly attenuated the scopolamine induced decrease in ELT on day 4 and TSTQ on day 5 (**Fig. 4** and **Fig. 5**).

2.10 *Effect of compound 7m on biochemical parameters*

After behavioral studies, biochemical parameters were determined in brain homogenates, as shown in **Table 3**, scopolamine administration significantly increased the TBARS levels and

AChE activity whereas endogenous antioxidant (reduced GSH) levels were significantly depleted as compared to vehicle treated animals.^{22,23}

The standard drug donepezil significantly reduced the TBARS levels and AChE activity whereas increased the GSH levels. Similar effects were observed in mice treated with most potent compound **7m** (2, 5 and 10 mg/kg, i.p). In the present investigation, scopolamine administration lead to enhanced oxidative stress showed by elevated TBARS levels and depleted reduced GSH levels in homogenate of mice brain. The TBARS and reduced GSH levels were restored with compound **7m** treatment significantly. These results showed that compound **7m** may attenuate the cognitive deficit by preventing the oxidative damage and neurodegeneration induced by scopolamine.

3. Experimental Section

3.1 Chemistry

All chemicals and solvents required for synthesis were obtained commercially from various suppliers and were of LR grade, used without any purification. The solvents were dehydrated according to standard methods. The synthesis was carried out using magnetic stirrer and hot plate (Perfit), and solvents were recovered using rotary vacuum evaporator (Perfit). The completion of each reaction was monitored by thin layer chromatography (DC-Alufolien (20x20 cm) Kieselgel 60 F₂₅₄ chromatoplates) using hexane:ethylacetate (6:4, v/v) and chloroform:methanol (9:1 v/v) as a TLC development solvent system. Impure compounds and intermediates were purified on silica columns from appropriate solvent. The melting points were recorded on an electronic melting point apparatus. The purity of all organic compounds was confirmed by TLC, IR, ¹H NMR, ¹³C NMR and Mass spectrometry. IR spectra were recorded on a Bruker (Alpha E) FT/IR spectrophotometer, ¹H-NMR spectra were recorded on a Bruker Advance II 400 MHz NMR spectrometer using chloroform (CDCl₃) or dimethylsulfoxide (DMSO-d₆) as solvent. The chemical shifts are reported in parts per million (δ) downfield from TMS and coupling constants are reported in hertz (Hz). Proton coupling patterns are abbreviated as single (s), double (d), triplet (t) and multiple (m). Mass spectra (ESI-MS) were recorded with a Waters, Q-TOF Micromass (LC-MS).

3.1.1 General procedures for the synthesis of intermediate *o*-Benzoyloxyacetophenone (3)

At first, the substituted *o*-Benzoyloxyacetophenone (**3**) was synthesized by stirring the mixture of substituted *o*-Hydroxyacetophenone (0.1mol) and substituted benzoyl chlorides (0.15mol) in dry pyridine. During the reaction, the mixture evolved spontaneous heat, and after about 15 minutes when the temperature comes down to room temperature, the mixture was poured, with constant stirring, into 3% hydrochloric acid containing crushed ice resulting in the precipitation of solid residue. The solid residue was then filtered and washed with methanol followed by water. The filtered residue was air dried, and re-crystallized from methanol resulting in the white precipitates of substituted *o*-Benzoyloxyacetophenone, yield 90%.

3.1.2 General procedures for the synthesis of intermediate *o*-Hydroxydibenzoylmethane (4)

To a warm solution of substituted *o*-Benzoyloxyacetophenone (**3**) in dry pyridine, hot pulverized 85% potassium hydroxide was added followed by mechanical stirring for 30 minutes resulting in the gradual appearance of yellowish brown precipitates of potassium salt of substituted *o*-Hydroxydibenzoylmethane (**4**). The reaction mixture was brought down to room temperature, and subsequently acidified with 10% acetic acid to desalt the compounds. The light-yellow precipitates of diketone (**4**) were filtered and dried, yield 85%.

3.1.3 General procedures for the synthesis of compounds 5(a-c).

The substituted *o*-Hydroxydibenzoylmethane (**4**), in the presence of glacial acetic acid and conc. sulphuric acid, was refluxed on water bath for 1h, to achieve the cyclized product. Then, the reaction mixture was poured onto crushed ice with vigorous stirring resulting in the precipitation of the compounds **5(a-c)**. The product was filtered, thoroughly washed with water to make it free from acid and dried. Then, purified on silica columns using hexane: ethyl acetate (6:4%) as solvent [38, 39]. (Scheme 1)

3.1.4 General procedures for the synthesis of intermediates 6(a-g)

The synthetic protocol for compound **6(a-g)** is outlined in Scheme 2. To synthesize the intermediates **6(a-g)**, anhydrous K₂CO₃ (10.0 mmol) and different α,ω -dibromoalkanes (4.0 mmol) were added to a solution of substituted compounds **5(a-c)** (2.0 mmol) in acetone (20 mL). After reflux for 10 h until the starting material disappeared, the solvent was removed under

vacuum; the residue was then poured into water and extracted with ethyl acetate. The solution was then dried over sodium sulphate and then concentrated. The intermediates **6(a-g)** were purified on silica columns using chloroform:methanol (9.5:0.5) [50]. (Scheme 2)

3.1.5 General procedures for the synthesis of final compounds 7(a-n).

To a solution of intermediates **6(a-g)** (0.5 mmol) in acetonitrile (10 mL), different amines (1.0 mmol) and anhydrous K_2CO_3 (2.5 mmol) were added. After stirring at 60°C for 12 h, the solvent was removed under vacuum; the mixture was diluted with $CHCl_3$ and then washed with water and brine. The organic layer was dried over Na_2SO_4 , filtered, concentrated in vacuo, and the final compounds **7(a-n)** were purified by column chromatography with $CHCl_3$:MeOH (95:5) elution [50]. (Scheme 3)

3.1.5.1. 7-hydroxy-2-(4-methoxyphenyl)-4H-chromen-4-one (5a):

Brown black, amorphous solid, yield 91%, m.p.: 231-236°C; IR (KBr) (cm^{-1}): (-OH) 3375 broad (s); (=C-H) str 3175 (m); (C=O) 1661 (s); 1626 Ar (C=C) str (m); 1H -NMR (400 MHz, DMSO- d_6 , δ ppm): 10.62 (1H, s, -OH), 7.94-7.96 (2H, dd, J = 1.88, 7.0 Hz, ArH), 7.89 (1H, d, J = 8.68 Hz, ArH), 7.05-7.08 (2H, d, J = 2.96 Hz, ArH), 6.94 (1H, d, J = 2.16 Hz, ArH), 6.87-6.90 (1H, dd, J = 2.20, 8.68 Hz, ArH), 6.69 (1H, s, ArH), 3.87 (3H, s, -OCH₃); (100 MHz, DMSO- d_6 , δ ppm): 176.36, 162.54, 162.01, 161.77, 157.36, 127.69, 126.25, 123.45, 116.07, 114.65, 114.24, 105.03, 102.34, 55.25; MS (ESI) m/z = 269.1 [M+H]⁺; R_f Value: 0.53 (Hexane: Ethyl acetate, 6:4).

3.1.5.2 2-(3,4-Dimethoxyphenyl)-7-hydroxy-4H-chromen-4-one (5b):

Light Yellow, Amorphous solid, yield 60%; IR (KBr) (cm^{-1}): 3375-3179 cm^{-1} (-OH, broad (s)); 1626 cm^{-1} (C=O, str, s); 1614 cm^{-1} (C=C, str, m); 1H -NMR (400 MHz, $CDCl_3$, δ ppm): 10.51 (1H, s-broad, -OH), 7.87-7.90 (1H, d, J = 8.72 Hz, ArH), 7.60-7.62 (1H, d, J = 7.12 Hz, ArH), 7.49 (1H, s, ArH), 7.06-7.08 (1H, d, J = 8.48 Hz, ArH), 6.95 (1H, s, ArH), 6.88-6.90 (1H, d, J = 7.88 Hz, ArH), 6.76 (1H, s, ArH), 3.93 (3H, s, -OCH₃), 3.90 (3H, s, -OCH₃); ^{13}C NMR (100 MHz, DMSO- d_6 , δ ppm): 176.36, 162.54, 161.39, 157.48, 149.8, 148.7, 126.30, 123.45, 121.47, 116.67, 114.87, 111.74, 108.47, 105.47, 102.50, 56.36; MS (ESI) m/z = 299.47 [M+H]⁺; R_f Value: 0.55 (Hexane:Ethyl acetate, 6:4).

3.1.5.3 7-hydroxy-2-(3,4,5-trimethoxyphenyl)-4H-chromen-4-one (5c)

Dark Brown, solid amorphous, yield 70%; IR (KBr) (cm^{-1}): 3674 cm^{-1} (-OH broad, s); 2926 cm^{-1} (=C-H, str, m); 1628 cm^{-1} (C=O, str, s); 1586 cm^{-1} (C=C, str, m); $^1\text{H-NMR}$ (400 MHz, DMSO- d_6 , δ ppm): 10.68 (1H, s-broad, -OH), 7.87-7.90 (1H, d, $J = 8.72$ Hz, ArH), 7.25 (2H, s, ArH), 6.99 (1H, s, ArH), 6.89-9.62 (1H, m, ArH), 6.87 (1H, s, ArH) 3.93 (6H, s, -OCH₃) 3.80 (3H, s, -OCH₃); (100 MHz, DMSO- d_6 , δ ppm): 176.54, 162.36, 161.71, 157.31, 153.01, 141.11, 126.30, 123.42, 116.02, 114.75, 105.11, 102.42, 61.03, 56.23; MS (ESI) $m/z = 329.1$ [M+H]⁺; R_f Value: 0.60 (Hexane:Ethyl acetate, 6:4).

3.1.5.4 7-(2-Bromopropoxy)-2-(4-methoxyphenyl)-4H-chromen-4-one (6a):

Light yellowish, solid amorphous, yield 55%; $^1\text{H-NMR}$ (400 MHz, CDCl₃, δ ppm): 8.10-8.13 (1H, d, $J = 9.40$ Hz, ArH), 7.87 (1H, s, ArH), 7.85-7.86 (1H, d, $J = 2.04$ Hz, ArH), 7.01-7.03 (2H, m, ArH), 6.96-6.98 (2H, m, ArH), 6.68 (1H, s, ArH), 4.23-4.26 (2H, t, -CH₂) 3.90-3.91 (2H, d, -CH₂), 3.89 (3H, s, -OCH₃) 2.09-2.15 (2H, m, -CH₂), R_f Value: 0.20 (CHCl₃: MeOH, 9:1).

3.1.5.5 7-(4-Bromobutoxy)-2-(4-methoxyphenyl)-4H-chromen-4-one (6b):

Yellow, solid amorphous, yield 75%; $^1\text{H-NMR}$ (400 MHz, CDCl₃, δ ppm): 8.11-8.13 (1H, d, $J = 8.64$ Hz, ArH), 7.83-7.87 (2H, m, ArH), 6.99-7.03 (2H, m, ArH), 6.67 (1H, s, ArH), 4.10-4.13 (2H, t, -CH₂), 3.88 (3H, s, -OCH₃), 3.49-3.53 (2H, t, -CH₂), 2.00-2.12 (4H, pentet, -CH₂). R_f Value: 0.65 (CHCl₃: MeOH, 9:1).

3.1.5.6 7-((5-Bromopentyl)oxy)-2-(4-methoxyphenyl)-4H-chromen-4-one (6c):

Yellowish cream, solid amorphous, yield 50%; $^1\text{H-NMR}$ (400 MHz, CDCl₃, δ ppm): 8.10-8.12 (1H, d, $J = 8.72$ Hz, ArH), 7.86-7.87 (1H, d, $J = 2.08$ Hz, ArH), 7.84-7.85 (1H, d, $J = 2.0$ Hz, ArH), 7.00-7.02 (2H, dd, $J = 6.92, 1.96$ Hz, ArH), 6.93-6.97 (2H, m, ArH), 6.68 (1H, s, ArH), 4.07-4.10 (2H, t, -CH₂), 3.88 (3H, s, -OCH₃), 3.44-3.47 (2H, t, -CH₂), 1.86-1.98 (4H, m, -CH₂), 1.67-1.69 (2H, m, -CH₂). R_f Value: 0.67 (CHCl₃: MeOH, 9:1).

3.1.5.7 7-((6-Bromohexyl)oxy)-2-(4-methoxyphenyl)-4H-chromen-4-one (6d):

Light yellowish brown, solid amorphous, yield 70%; $^1\text{H-NMR}$ (400 MHz, DMSO- d_6 , δ ppm): 8.00-8.02 (2H, d, $J = 8.88$ Hz, ArH), 7.92-7.94 (1H, d, $J = 8.80$ Hz, ArH), 7.25-7.26 (1H, d, $J = 2.28$ Hz, ArH), 7.08-7.10 (2H, d, $J = 8.88$ Hz, ArH), 7.00-7.03 (1H, dd, $J = 8.80$ Hz, ArH), 6.79 (1H, s, ArH), 4.22-4.25 (2H, t, $-\text{CH}_2$) 3.87 (3H, s, $-\text{OCH}_3$) 2.75-2.81 (5H, m, $-\text{CH}_2$, -NH), 2.52-2.53 (6H, t, $-\text{CH}_2$) R_f Value: 0.70 (CHCl_3 : MeOH, 9:1).

3.1.5.8. 7-((8-Bromooctyl)oxy)-2-(4-methoxyphenyl)-4H-chromen-4-one (6e):

Light yellowish, solid amorphous, yield 75%; $^1\text{H-NMR}$ (400 MHz, CDCl_3 , δ ppm): 8.03-8.05 (1H, d, $J = 8.76$ Hz, ArH), 7.77.80 (2H, m, ArH), 6.95-6.96 (1H, t, ArH), 6.93-6.94 (1H, d, $J = 1.88$ Hz, ArH), 6.86-6.90 (2H, m, ArH), 6.60 (1H, s, ArH), 3.98-4.01 (2H, t, $-\text{CH}_2$), 3.82 (3H, s, $-\text{OCH}_3$), 3.34-3.36 (2H, t, $-\text{CH}_2$), 1.74-1.97 (4H, m, $-\text{CH}_2$), 1.32-1.45 (8H, m, $-\text{CH}_2$). R_f Value: 0.65 (CHCl_3 : MeOH, 9:1). R_f Value: 0.68 (CHCl_3 : MeOH, 9:1).

3.1.5.9. 7-(3-Bromopropoxy)-2-(3,4-dimethoxyphenyl)-4H-chromen-4-one (6f):

Yellow, solid amorphous, yield 55%; $^1\text{H-NMR}$ (400 MHz, CDCl_3 , δ ppm): 8.12--8.15 (1H, d, $J = 9.48$ Hz, ArH), 7.53-7.56 (1H, dd, $J = 8.52, 2.08$ Hz, ArH), 7.37 (2H, t, $J = 2.12$ Hz, ArH), 6.97-6.99 (2H, dd, $J = 7.2, 1.04$ Hz, ArH), 6.70 (1H, s, ArH), 4.23-4.26 (2H, t, $-\text{CH}_2$), 3.99 (3H, s, $-\text{OCH}_3$), 3.97 (3H, s, $-\text{OCH}_3$), 3.62-3.66 (2H, t, $-\text{CH}_2$), 3.38-3.41 (2H, pentet, $-\text{CH}_2$). R_f Value: 0.65 (CHCl_3 : MeOH, 9:1).

3.1.5.10. 7-(2-Bromoethoxy)-2-(3,4,5-trimethoxyphenyl)-4H-chromen-4-one (6g):

Light yellow, solid amorphous, yield 58%; $^1\text{H-NMR}$ (400 MHz, CDCl_3 , δ ppm): 8.15--8.17 (1H, d, $J = 8.64$ Hz, ArH), 7.11 (2H, s, ArH), 6.99-7.00 (2H, t, $J = 2.48, 4.72$ Hz, ArH), 6.72 (1H, s, ArH), 4.41-4.44 (2H, t, $-\text{CH}_2$), 3.96 (6H, s, $-\text{OCH}_3$), 3.93 (3H, s, $-\text{OCH}_3$), 3.69-3.72 (2H, t, $-\text{CH}_2$). R_f Value: 0.67 (CHCl_3 : MeOH, 9:1).

3.1.5.11. 2-(4-Methoxyphenyl)-7-(3-(4-methylpiperidin-1-yl)propoxy)-4H-chromen-4-one (7a):

Greyish brown, solid amorphous, yield 55%; IR (KBr) (cm^{-1}): 1625 cm^{-1} (C=O, str, s), 1595 cm^{-1} (C=C, s), 1250 cm^{-1} (C-O, asym., s), 1355 cm^{-1} (C-N, str, s); $^1\text{H-NMR}$ (400 MHz, CDCl_3 , δ ppm): 8.09-8.11 (1H, d, $J = 9.4$ Hz, ArH), 7.84-7.86 (2H, d, $J = 10.4$ Hz, ArH), 7.02 (1H, s, ArH), 7.00 (1H, s, ArH), 6.94-6.96 (2H, m, ArH), 6.67 (1H, s, ArH), 4.12-4.15 (2H, t, -

CH_2), 3.88 (3H, s, $-OCH_3$) 3.00-3.03 (2H, t, $-CH_2$), 2.59-2.63 (2H, t, $-CH_2$), 2.03-2.11 (4H, m, $-CH_2$), 1.65-1.68 (2H, t, $-CH_2$), 1.32-1.41 (3H, m, $-CH$, $-CH_2$) 1.22-1.28 (4H, m, $-CH_2$), 0.93-0.95 (3H, d, $-CH_3$); ^{13}C NMR (100 MHz, $CDCl_3$): 177.91, 163.40, 163.08, 162.25, 157.87, 127.86, 126.96, 124.15, 117.73, 114.58, 106.09, 101.91, 66.95, 55.21, 53.87, 33.70, 30.55, 26.26, 21.73; $m/z = 408.45 [M+H]^+$; R_f Value: 0.23 ($CHCl_3$: MeOH, 9:1).

3.1.5.12. 7-(3-(4-(2-Hydroxyethyl)piperazin-1-yl)propoxy)-2-(4-methoxyphenyl)-4H-chromen-4-one (7b):

Light yellowish brown, solid amorphous, yield 78%; IR (KBr) (cm^{-1}): 3299 cm^{-1} (OH, str, s), 1630 cm^{-1} (C=O, str, s), 1597 cm^{-1} (C=C, str, s), 1252 cm^{-1} (C-O, asym., s), 1375 cm^{-1} (C-N, str, s); 1H -NMR (400 MHz, $CDCl_3$, δ ppm): 8.02-8.04 (1H, d, $J = 9.4$ Hz, ArH), 7.77-7.79 (2H, d, $J = 8.88$ Hz, ArH), 6.92-6.95 (2H, s, ArH), 6.90 (1H, d, $J = 2.28$ Hz, ArH), 6.60 (1H, s, ArH), 4.52 (1H, s-broad, $-OH$), 4.05-4.08 (2H, t, $-CH_2$), 3.81 (3H, s, $-OCH_3$), 3.54-3.57 (2H, m, $-CH_2$), 2.46-2.50 (8H, m, $-CH_2$), 2.19-2.21 (4H, t, $-CH_2$), 1.94-1.98 (2H, pentet, $-CH_2$); ^{13}C NMR (100 MHz, $CDCl_3$): 177.94, 163.49, 163.09, 162.26, 157.90, 127.86, 126.97, 124.14, 117.70, 114.55, 114.43, 106.09, 100.94, 66.85, 59.25, 57.73, 55.52, 53.23, 52.83, 26.51; MS (ESI) $m/z = 439.42 [M+H]^+$; R_f Value: 0.35 ($CHCl_3$: MeOH, 9:1).

3.1.5.13. 2-(4-Methoxyphenyl)-7-(4-(4-methylpiperidin-1-yl)butoxy)-4H-chromen-4-one (7c):

Greyish brown, solid amorphous, yield 55%; IR (KBr) (cm^{-1}): 1629 cm^{-1} (C=O, str, s), 1597 cm^{-1} (C=C, s), 1252 cm^{-1} (C-O, asym., s), 1354 cm^{-1} (C-N, str, s); 1H -NMR (400 MHz, $CDCl_3$, δ ppm): 8.10-8.12 (1H, d, $J = 8.76$ Hz, ArH), 7.84-7.87 (2H, m, ArH), 7.00-7.03 (2H, m, ArH), 6.93-6.97 (2H, m, ArH), 6.67 (1H, s, ArH), 4.08-4.11 (2H, t, $-CH_2$), 3.88 (3H, s, $-OCH_3$) 2.94-2.91 (2H, t, $-CH_2$), 2.39-2.42 (2H, t, $-CH_2$), 1.62-1.98 (8H, m, $-CH_2$) 1.21-1.34 (3H, m, $-CH_2$, $-CH$), 0.91-0.93 (3H, d, $-CH_3$); ^{13}C NMR (100 MHz, $CDCl_3$): 177.94, 163.50, 163.06, 162.22, 157.89, 127.85, 126.92, 124.12, 117.62, 114.57, 114.41, 106.04, 100.84, 68.41, 58.45, 55.50, 53.94, 34.03, 30.72, 27.15, 23.36, 21.83; MS (ESI) $m/z = 422.51 [M+H]^+$; R_f Value: 0.28 ($CHCl_3$: MeOH, 9:1).

3.1.5.14. 7-(4-(4-(2-Hydroxyethyl)piperazin-1-yl)butoxy)-2-(4-methoxyphenyl)-4H-chromen-4-one (7d):

Light yellowish grey, solid amorphous, yield 70%; IR (KBr) (cm^{-1}): 3356 cm^{-1} (OH, str, s), 1627 cm^{-1} (C=O, str, s), 1599 cm^{-1} (C=C, str, s), 1253 cm^{-1} (C-O, asym., s), 1370 cm^{-1} (C-N, str, s); $^1\text{H-NMR}$ (400 MHz, CDCl_3 , δ ppm): 8.10-8.12 (1H, d, $J = 8.72$ Hz, *ArH*), 7.86-7.87 (1H, d, $J = 2.09$ Hz, *ArH*), 7.85 (1H, d, $J = 2.08$ Hz, *ArH*), 7.01-7.03 (2H, m, *ArH*), 6.93-6.97 (2H, m, *ArH*), 6.68 (1H, s, *ArH*), 4.27 (1H, s-broad, -OH), 4.08-4.12 (2H, t, - CH_2), 3.89 (3H, s, - OCH_3), 3.60-3.62 (2H, t, - CH_2), 2.53-2.56 (8H, m, - CH_2), 2.41-2.45 (2H, t, - CH_2) 1.86-1.90 (2H, t, - CH_2), 1.68-1.74 (4H, pentet, - CH_2); $^{13}\text{C NMR}$ (100 MHz, CDCl_3): 176.38, 162.99, 162.29, 161.87, 157.34, 127.70, 126.02, 123.32, 117.00, 114.42, 114.23, 105.02, 100.93, 68.02, 56.75, 55.25, 52.13, 51.39, 26.18, 22.21; ; MS (ESI) $m/z = 453.44$ $[\text{M}+\text{H}]^+$; R_f Value: 0.37 (CHCl_3 : MeOH, 9:1).

3.1.5.15. 2-(4-Methoxyphenyl)-7-((5-(4-methylpiperidin-1-yl)pentyl)oxy)-4H-chromen-4-one (7e):

Brown, solid amorphous, yield 60%; IR (KBr) (cm^{-1}): 1625 cm^{-1} (C=O, str, s), 1597 cm^{-1} (C=C, s), 1245 cm^{-1} (C-O, asym., s), 1366 cm^{-1} (C-N, str, s); $^1\text{H-NMR}$ (400 MHz, CDCl_3 , δ ppm): 8.10-8.12 (1H, d, $J = 8.76$ Hz, *ArH*), 7.78-7.80 (2H, d, $J = 8.8$ Hz, *ArH*), 7.93-7.95 (2H, d, $J = 8.8$ Hz, *ArH*), 6.86-6.88 (2H, d, $J = 6.92$ Hz, *ArH*), 6.65 (1H, s, *ArH*), 4.08-4.11 (2H, t, - CH_2), 3.88 (3H, s, - OCH_3) 3.45-3.48 (2H, t, - CH_2), 2.83-2.87 (2H, t, - CH_2), 2.49-2.51 (2H, t, - CH_2), 1.73-1.83 (6H, m, - CH_2) 1.45-1.61 (5H, m, - CH_2), 0.91-0.93 (3H, d, - CH_3); $^{13}\text{C NMR}$ (100 MHz, CDCl_3): 177.94, 163.32, 163.18, 162.29, 157.91, 127.89, 126.94, 124.02, 117.71, 114.59, 114.41, 105.98, 100.86, 67.93, 56.71, 55.51, 50.14, 34.07, 29.69, 28.40, 23.48, 21.17; MS (ESI) $m/z = 436.48$ $[\text{M}+\text{H}]^+$; R_f Value: 0.27 (CHCl_3 : MeOH, 9:1).

3.1.5.16. 7-((5-(4-(2-Hydroxyethyl)piperazin-1-yl)pentyl)oxy)-2-(4-methoxyphenyl)-4H-chromen-4-one (7f):

Light grey, solid amorphous, yield 50%; IR (KBr) (cm^{-1}): 3401 cm^{-1} (OH, str, s), 1628 cm^{-1} (C=O, str, s), 1599 cm^{-1} (C=C, str, s), 1252 cm^{-1} (C-O, asym., s), 1360 cm^{-1} (C-N, str, s); $^1\text{H-NMR}$ (400 MHz, CDCl_3 , δ ppm): 8.09-8.11 (1H, d, $J = 8.72$ Hz, *ArH*), 7.84-7.86 (2H, d, $J = 8.92$ Hz, *ArH*), 7.02 (1H, s, *ArH*), 7.02 (1H, s, *ArH*), 7.00 (1H, s, *ArH*), 6.92-6.96 (2H, m, *ArH*), 6.67 (1H, s, *ArH*), 4.32 (1H, s-broad, -OH), 4.05-4.08 (2H, t, - CH_2), 3.88 (3H, s, - OCH_3), 3.60-3.62 (2H, t, - CH_2), 2.53-2.56 (2H, t, - CH_2), 2.37-2.40 (3H, t, - CH_2), 1.70-1.90 (8H, t, - CH_2), 1.51-

1.59 (6H, m, $-CH_2$); ^{13}C NMR (100 MHz, $CDCl_3$): 177.92, 163.55, 163.06, 162.24, 157.90, 127.84, 126.93, 124.13, 117.62, 114.54, 114.41 106.06, 100.86, 68.48, 59.27, 58.23, 57.60, 55.50, 52.61, 52.30, 29.68, 28.89, 27.11; MS (ESI) $m/z = 467.47 [M+H]^+$; R_f Value: 0.32 ($CHCl_3$: MeOH, 9:1).

3.1.5.17. 2-(4-Methoxyphenyl)-7-((6-(4-methylpiperidin-1-yl)hexyl)oxy)-4H-chromen-4-one (7g):

Grey, solid amorphous, yield 55%; IR (KBr) (cm^{-1}): 1628 cm^{-1} (C=O, str, s), 1598 cm^{-1} (C=C, s), 1251 cm^{-1} (C-O, asym., s), 1365 cm^{-1} (C-N, str, s); 1H -NMR (400 MHz, $CDCl_3$, δ ppm): 8.09-8.11 (1H, d, $J = 8.56$ Hz, *ArH*), 7.84-7.87 (2H, d, $J = 8.76$ Hz, *ArH*), 7.00-7.02 (2H, m, *ArH*), 6.93-6.95 (2H, m, *ArH*), 6.67 (1H, s, *ArH*), 4.04-4.07 (2H, t, $-CH_2$), 3.88 (3H, s, $-OCH_3$) 3.20-3.22 (2H, t, $-CH_2$), 2.61-2.65 (2H, t, $-CH_2$), 2.23-2.28 (2H, t, $-CH_2$), 1.82-1.86 (2H, t, $-CH_2$), 1.70-1.72 (3H, m, $-CH_2$, $-CH$), 1.22-1.44 (8H, m, $-CH_2$), 0.95-0.97 (3H, d, $-CH_3$); ^{13}C NMR (100 MHz, $CDCl_3$): 177.92, 163.52, 163.07, 162.25, 157.92, 127.86, 126.93, 124.14, 117.65, 114.57, 114.43, 106.06, 100.85, 68.40, 57.51, 55.51, 32.10, 29.88, 29.71 28.80, 26.95, 25.05, 21.26; MS (ESI) $m/z = 450.49 [M+H]^+$; R_f Value: 0.28 ($CHCl_3$: MeOH, 9:1).

3.1.5.18. 7-((6-(4-(2-Hydroxyethyl)piperazin-1-yl)hexyl)oxy)-2-(4-methoxyphenyl)-4H-chromen-4-one (7h):

Greyish brown, solid amorphous, yield 60%; IR (KBr) (cm^{-1}): 3328 cm^{-1} (OH, str, s), 1623 cm^{-1} (C=O, str, s), 1594 cm^{-1} (C=C, str, s), 1252 cm^{-1} (C-O, asym., s), 1356 cm^{-1} (C-N, str, s); 1H -NMR (400 MHz, $CDCl_3$, δ ppm): 8.08-8.10 (1H, d, $J = 8.72$ Hz, *ArH*), 7.82-7.86 (2H, m, *ArH*), 6.99-7.02 (2H, m, *ArH*), 6.91-6.96 (2H, m, *ArH*), 6.66 (1H, s, *ArH*), 4.35 (1H, s-broad, $-OH$), 4.03-4.07 (2H, t, $-CH_2$), 3.87 (3H, s, $-OCH_3$), 3.63-3.66 (2H, t, $-CH_2$), 2.59-2.66 (8H, m, $-CH_2$), 2.42-2.46 (2H, t, $-CH_2$), 1.80-1.85 (2H, pentet, $-CH_2$), 1.47-1.59 (8H, m, $-CH_2$); ^{13}C NMR (100 MHz, $CDCl_3$): 177.90, 163.48, 163.03, 162.21, 157.97, 127.87, 126.90, 124.18, 117.67, 114.58, 114.44, 106.02, 100.89, 68.53, 59.30, 58.28, 57.48, 55.52, 52.71, 52.12, 29.74, 28.82, 27.10, 25.42; MS (ESI) $m/z = 481.49 [M+H]^+$; R_f Value: 0.31 ($CHCl_3$: MeOH, 9:1).

3.1.5.19. 2-(4-Methoxyphenyl)-7-((8-(4-methylpiperidin-1-yl)octyl)oxy)-4H-chromen-4-one (7i):

Light grey, solid amorphous, yield 65%; IR (KBr) (cm^{-1}): 1625 ($\text{C}=\text{O}$, str, s), 1598 cm^{-1} ($\text{C}=\text{C}$, s), 1254 cm^{-1} ($\text{C}-\text{O}$, asym., s), 1368 cm^{-1} ($\text{C}-\text{N}$, str, s); ^1H -NMR (400 MHz, CDCl_3 , δ ppm): 8.09-8.11 (1H, d, $J = 8.68$ Hz, *ArH*), 7.86 (1H, d, $J = 1.96$ Hz, *ArH*), 7.84 (1H, d, $J = 1.92$ Hz, *ArH*), 7.00-7.02 (2H, m, *ArH*), 6.93-6.96 (2H, m, *ArH*), 6.67 (1H, s, *ArH*), 4.04-4.07 (2H, t, $-\text{CH}_2$), 3.88 (3H, s, $-\text{OCH}_3$), 3.14-3.17 (2H, d, $-\text{CH}_2$), 2.54-2.58 (2H, t, $-\text{CH}_2$), 2.21-2.24 (2H, t, $-\text{CH}_2$), 1.90 (1H, m, $-\text{CH}$), 1.81-1.84 (2H, m, $-\text{CH}_2$), 1.63-1.71 (4H, m, $-\text{CH}_2$), 1.32-1.36 (10H, m, $-\text{CH}_2$), 0.94-0.96 (3H, d, $-\text{CH}_3$); ^{13}C NMR (100 MHz, CDCl_3): 177.92, 163.60, 163.03, 162.22, 157.91, 127.84, 126.90, 124.17, 117.60, 114.57, 114.41, 106.07, 100.83, 68.59, 58.26, 55.49, 53.35, 32.51, 31.63, 29.69, 29.35, 28.92, 27.24, 25.47, 21.36; MS (ESI) $m/z = 478.50$ [$\text{M}+\text{H}$] $^+$; R_f Value: 0.25 (CHCl_3 : MeOH, 9:1).

3.1.5.20. 7-((8-(4-(2-Hydroxyethyl)piperazin-1-yl)octyl)oxy)-2-(4-methoxyphenyl)-4H-chromen-4-one (7j):

Light greyish, solid amorphous, yield 70%; IR (KBr) (cm^{-1}): 3328 (OH , str, s), 1622 cm^{-1} ($\text{C}=\text{O}$, str, s), 1597 cm^{-1} ($\text{C}=\text{C}$, str, s), 1252 cm^{-1} ($\text{C}-\text{O}$, asym., s), 1357 cm^{-1} ($\text{C}-\text{N}$, str, s); ^1H -NMR (400 MHz, CDCl_3 , δ ppm): 8.09-8.11 (1H, d, $J = 8.76$ Hz, *ArH*), 7.86 (1H, d, $J = 1.96$ Hz, *ArH*), 7.84 (1H, d, $J = 1.96$ Hz, *ArH*), 6.99-7.02 (2H, m, *ArH*), 6.92-6.97 (2H, m, *ArH*), 6.67 (1H, s, *ArH*), 4.04-4.07 (2H, t, $-\text{CH}_2$), 3.88 (3H, s, $-\text{OCH}_3$), 3.60-3.63 (2H, t, $-\text{CH}_2$), 3.10-3.13 (2H, t, $-\text{CH}_2$), 2.55-2.57 (8H, t, $-\text{CH}_2$), 2.34-2.38 (2H, t, $-\text{CH}_2$), 1.81-1.85 (2H, pentet, $-\text{CH}_2$), 1.31-1.36 (10H, m, $-\text{CH}_2$); ^{13}C NMR (100 MHz, CDCl_3): 177.96, 163.63, 163.07, 162.25, 157.93, 127.85, 126.94, 124.16, 117.59, 114.59, 114.42, 106.07, 100.84, 68.65, 59.28, 58.60, 57.68, 55.50, 52.98, 52.62, 29.70, 29.52, 28.98, 27.47, 25.92; MS (ESI) $m/z = 509.50$ [$\text{M}+\text{H}$] $^+$; R_f Value: 0.34 (CHCl_3 : MeOH, 9:1).

3.1.5.21. 2-(3,4-Dimethoxyphenyl)-7-(2-(4-methylpiperidin-1-yl)ethoxy)-4H-chromen-4-one (7k):

Light yellow, solid amorphous, yield 50%; IR (KBr) (cm^{-1}): 1627 ($\text{C}=\text{O}$, str, s), 1596 cm^{-1} ($\text{C}=\text{C}$, s), 1259 cm^{-1} ($\text{C}-\text{O}$, asym., s), 1366 cm^{-1} ($\text{C}-\text{N}$, str, s); ^1H -NMR (400 MHz, CDCl_3 , δ ppm): 8.15-8.18 (1H, d, $J = 8.76$ Hz, *ArH*), 7.36-7.37 (1H, d, $J = 1.68$ Hz, *ArH*), 7.19 (1H, s, *ArH*), 6.90-6.92 (3H, m, *ArH*), 6.62 (1H, s, *ArH*), 4.07-4.09 (2H, t, $-\text{CH}_2$), 3.91 (3H, s, $-\text{OCH}_3$), 3.90 (3H, s, $-\text{OCH}_3$), 2.69-2.73 (2H, t, $-\text{CH}_2$), 1.87-2.01 (4H, m, $-\text{CH}_2$), 1.19-1.31 (5H,

m, $-CH_2$, $-CH$), 0.84-0.86 (3H, d, $-CH_3$); ^{13}C NMR (100 MHz, $CDCl_3$): 177.91, 163.40, 162.93, 157.87, 149.81, 148.06, 127.09, 122.9, 121.07, 117.83, 114.81, 111.9, 107.06, 103.10, 101.17, 66.71, 58.77, 56.40, 54.53, 34.12, 31.81, 21.85; MS (ESI) m/z = 424.49 $[M+H]^+$; R_f Value: 0.22 ($CHCl_3$: MeOH, 9:1).

3.1.5.22. 2-(3,4-Dimethoxyphenyl)-7-(3-(4-methylpiperidin-1-yl)propyl)-4H-chromen-4-one (7l):

Light yellow, solid amorphous, yield 50%; IR (KBr) (cm^{-1}): 1623 cm^{-1} (C=O, str, s), 1592 cm^{-1} (C=C, s), 1257 cm^{-1} (C-O, asym., s), 1362 cm^{-1} (C-N, str, s); 1H -NMR (400 MHz, $CDCl_3$, δ ppm): 8.03-8.06 (1H, d, J = 9.4 Hz, ArH), 7.46-7.48 (1H, dd, J = 8.44, 2.12 Hz, ArH), 7.30 (1H, d, J = 2.12 Hz, ArH), 6.89-6.92 (3H, m, ArH), 6.62 (1H, s, ArH), 4.06-4.09 (2H, t, $-CH_2$), 3.92 (3H, s, $-OCH_3$), 3.90 (3H, s, $-OCH_3$), 2.44-2.48 (2H, t, $-CH_2$), 1.96-2.00 (2H, t, $-CH_2$), 1.87-1.92 (5H, t, $-CH_2$), 1.18-1.30 (5H, m, $-CH_2$, CH), 0.85-0.87 (3H, d, $-CH_3$); ^{13}C NMR (100 MHz, $CDCl_3$): 177.79, 163.30, 162.97, 157.98, 149.52, 148.25, 127.03, 122.2, 121.05, 117.87, 114.72, 112.6, 107.31, 103.72, 100.96, 66.76, 58.71, 56.43, 53.51, 32.81, 31.96, 25.63, 21.45; MS (ESI) m/z = 438.55 $[M+H]^+$; 478.62 $[M+K]^+$; R_f Value: 0.26 ($CHCl_3$: MeOH, 9:1).

3.1.5.23. 7-(2-(4-Methylpiperidin-1-yl)ethoxy)-2-(3,4,5-trimethoxyphenyl)-4H-chromen-4-one (7m):

Light grey, solid amorphous, yield 55%; IR (KBr) (cm^{-1}): 1625 cm^{-1} (C=O, str, s), 1595 cm^{-1} (C=C, s), 1248 cm^{-1} (C-O, asym., s), 1357 cm^{-1} (C-N, str, s); 1H -NMR (400 MHz, $CDCl_3$, δ ppm): 8.10-8.13 (1H, d, J = 9.62 Hz, ArH), 7.11 (2H, s, ArH), 7.00 (1H, d, J = 9.56 Hz, ArH), 6.98 (1H, s, ArH), 6.71 (1H, s, ArH), 4.23-4.26 (2H, t, $-CH_2$), 3.96 (6H, s, $-OCH_3$), 3.93 (3H, s, $-OCH_3$), 2.86-2.89 (2H, t, $-CH_2$), 2.13-2.19 (2H, t, $-CH_2$), 1.31-1.41 (6H, m, $-CH_2$), 0.93-0.94 (3H, d, $-CH_3$) 0.86-0.89 (1H, m, $-CH$); ^{13}C NMR (100 MHz, $CDCl_3$): 177.81, 163.35, 162.89, 157.89, 153.56, 141.04, 127.09, 127.02, 117.79, 114.85, 107.03, 103.60, 101.11, 66.67, 61.05, 57.12, 56.36, 54.47, 34.01, 30.45, 21.80; MS (ESI) m/z = 454.56 $[M+H]^+$; R_f Value: 0.22 ($CHCl_3$: MeOH, 9:1).

3.1.5.24. 7-(3-(4-Methylpiperidin-1-yl)propoxy)-2-(3,4,5-trimethoxyphenyl)-4H-chromen-4-one (7n):

Light Brown, solid amorphous, yield 50%; IR (KBr) (cm^{-1}): 1627 cm^{-1} (C=O, str, s), 1595 cm^{-1} (C=C, s), 1241 cm^{-1} (C-O, asym., s), 1350 cm^{-1} (C-N, str, s); $^1\text{H-NMR}$ (400 MHz, CDCl_3 , δ ppm): 8.09-8.11 (1H, d, $J = 8.4$ Hz, *ArH*), 7.10 (2H, s, *ArH*), 6.94-6.96 (2H, d, $J = 8.76$ Hz, *ArH*), 6.98 (1H, s, *ArH*), 6.70 (1H, s, *ArH*), 4.02-4.21 (2H, t, $-\text{CH}_2$), 3.95 (6H, s, $-\text{OCH}_3$), 3.91 (3H, s, $-\text{OCH}_3$), 2.73-2.71 (2H, t, $-\text{CH}_2$), 2.20-2.23 (4H, t, $-\text{CH}_2$), 1.23-1.71 (6H, m, $-\text{CH}_2$, $-\text{CH}$), 0.90-0.95 (3H, d, $-\text{CH}_3$); $^{13}\text{C NMR}$ (100 MHz, CDCl_3): 177.83, 163.34, 162.95, 157.92, 153.58, 141.06, 127.05, 117.81, 114.78, 107.29, 103.61, 100.99, 66.74, 61.06, 56.38, 54.97, 53.49, 32.75, 31.92, 25.56, 21.81; MS (ESI) $m/z = 468.55$ $[\text{M}+\text{H}]^+$; R_f Value: 0.25 (CHCl_3 : MeOH, 9:1).

3.2 Biological activity

3.2.1. *In vitro* inhibition of Acetylcholinesterase Enzyme

The inhibitory potency of target compounds on brain AChE was determined using spectroscopic method at 450 nm by the method of Ellman *et al.* with slight modification [40]. The potency of synthesized compounds was expressed as IC_{50} with donepezil as standard acetylcholinesterase inhibitor. Each concentration was analyzed in triplicate. Data from concentration–inhibition experiments of the inhibitors were calculated by nonlinear regression analysis, using the GraphPad Prism 5 program.

3.2.2. *In vitro* advanced glycation end-product (AGEs) formation inhibitory activity

The assay for the ability of the flavone to inhibit the glucose-mediated protein glycation and the development of fluorescent AGEs was performed. Different concentrations of various compounds were prepared by dissolving in DMSO. Anti-glycation assay was performed according to the methods reported by Matsuura and colleagues with slight modification.¹¹ The Fluorescence was measured spectrofluorometrically (LS-55 (Perkin Elmer) at 370 nm (excitation) and 440 nm (emission). Aminoguanidine was used as a positive control. All experiments were performed in triplicate.

3.2.3. DPPH radical scavenging activity method

The stable 1, 1-diphenyl-2-picryl hydrazyl radical (DPPH) was used for determination of free radical-scavenging activity of the test compounds by widely used Blois *et.al.* method.¹² The

absorbance was recorded at 517 nm spectrophotometrically. Ascorbic acid was used as standard. IC_{50} values denote the concentration of sample, which is required to scavenge 50% of DPPH free radicals.

3.2.4. Kinetic characterization of AChE inhibition

The kinetics studies were performed using the Ellman's method with three different concentrations (0.01, 0.05 and 0.1 μ M) of compound **7m**. The Lineweaver–Burk reciprocal plots were constructed by plotting the inverse initial velocity ($1/V$) as a function of the inverse of the substrate concentration ($1/[S]$) at varying concentrations of the substrate acetylthiocholine (0.05–0.5 mM). The parallel control experiments were achieved without inhibitor in the assay. The double reciprocal plots were evaluated by a weighted least-squares analysis. Each experiment was performed in triplicate.

3.2.5. Molecular docking studies

To understand the binding interactions and selectivity of our synthesized compounds against AChE, molecular docking simulation was carried out with Glide program of Schrödinger software. The compounds showing good anti-cholinesterase activity were sketched and cleaned in maestro molecular modeling workspace followed by energy minimization in 'ligprep' program of Schrödinger software using OPLS_2005 force field at pH of 7.4.¹⁴ The X-ray crystallographic structure of AChE complex with donepezil (PDB code 1EVE) was obtained from the Protein Data Bank (<http://www.rcsb.org/pdb>) and optimized for docking analysis.¹⁵ The optimization protocol includes addition of hydrogen atoms, deletion of water molecules, completion of bond orders, assignment of hydrogen bonds and complex minimization to RMSD of 0.20Å using OPLS_2005 force field. The active molecules were docked into the active site of the protein using extra precision (XP) docking mode of 'glide' program.¹⁶

3.2.6. Molecular Dynamic Simulations

The molecule with the highest inhibitory activity docked with the AChE protein was used in molecular dynamics simulations (10 ns) using Desmond molecular dynamics module of Schrodinger.¹⁷ The simulations aided to stabilize the protein-ligand complex and analyze the most probable interaction by studying its simulation–interaction diagram. From this analysis, the important interactions for ligand were assessed and can be utilized for further identification. For

molecular dynamics simulations, the system was first built using the TIP3P solvent model with orthorhombic box shape; the pH was adjusted by adding Na⁺ ions, and the salt concentration was set at 0.15 M. The simulation was carried out using the NPT ensemble and a time step of 1.0 fs; the temperature was fixed at 310 K using the Nose-Hoover Chain method as the thermostat and pressure of 1.01325 bar using Martyn–Tobias–Klein as the barostat.

3.2.7. ADME property prediction

To investigate the potential of the new compounds as anti-AD agents, their ADME (Absorption, Distribution, Metabolism and Excretion) properties were predicted using QikProp program, v. 3.5 of the Schrödinger software.¹⁸ This provided an estimate of the physicochemical properties and the bioavailability of the compounds. Various parameters such as polar surface area (PSA), solvent accessible surface area (SASA), QPPCaco (predicted apparent Caco-2 cell permeability in nm/s, CNS activity (predicted central nervous system activity on a -2 (inactive) to +2 (active) scale), QPlogBB (predicted brain/blood partition coefficient), Caco-2 cells is a model for the gut blood barrier), QPPMDCK (predicted apparent MDCK cell permeability in nm/s. MDCK cells are considered to be a good mimic for the blood–brain barrier), QPlogS (predicted aqueous solubility), QPlogKhsa (prediction of binding to human serum albumin), and percent human oral absorption (predicted human oral absorption on 0–100% scale) were calculated. The acceptability of the compounds based on the Lipinski's rule of five was also estimated from the results.¹⁹

3.3. *In vivo* assay

3.3.1. Experimental Animals

Swiss albino mice of either sex, weighing 20–25 g (procured from Central Research Institute, Kasauli, Himachal Pradesh, India) were used for *in vivo* evaluation of learning and memory. The experimental protocol was approved by the Institutional Animal Ethics Committee (IAEC). The animals were housed in the Animal house facility, Punjabi University Patiala, India and the care of the animals was carried out as per the guidelines of the Committee for the Purpose of Control and Supervision of Experiments on Animals (CPCSEA), Ministry of Environment and Forest, Government of India (Reg. No. 107/1999/CPCSEA).

3.3.2. Drugs and chemicals

Scopolamine bromide was dissolved in normal saline and test drug was dissolved in 10% dimethylsulfoxide (DMSO). All other reagents used in the present study were of analytical grade and freshly prepared.

3.3.3. Assessment of learning and memory by Morris water maze

Morris water maze is one of the most commonly used animal models to test memory.²¹ It consists of large circular pool and is divided in to four quadrants (Q1, Q2, Q3, and Q4). Each animal was subjected to trial of 120 s in the water maze for five consecutive days and the memory was assessed in terms of: (i) escape latency time (ELT), that is, the time taken by the animal to locate the hidden platform in the target quadrant (Q4) for the first 4 days of training, (ii) time spent in target quadrant (Q4) on fifth day of trial, that is, the day of retrieval.

3.3.4. Experimental protocol

Six groups, each group comprising five Swiss albino mice, were employed in the present study.

3.3.4.1. Group I: normal control.

Normal mice, without any treatment, were subjected to trials on the water maze for 5 days to note escape latency time (ELT) for first 4 days (an index of learning) and time spent in target quadrant (TSTQ) on fifth day of trial (an index of retrieval).

3.3.4.2. Group II: scopolamine in vehicle treated control.

Scopolamine (0.5 mg/kg) in 10% DMSO, vehicle treated control was administered in scopolamine treated mice (30 min prior to scopolamine administration) to each mouse before subjecting to first four trials and rest of the procedure was same as described in group I.

3.3.4.3. Group III: Donepezil in scopolamine treated control.

Donepezil (2 mg/kg) was administered in scopolamine treated mice (30 min prior to scopolamine administration) to each.

3.3.4.4. Group IV, V and VI: test compound (7m) (2, 5, and 10 mg/kg) in scopolamine treated control.

The test compound with most potent acetylcholinesterase inhibitory activity (**7m**) was administered in scopolamine treated mice (30 min prior to scopolamine administration) to each mouse before subjecting to first four trials and rest of the procedure was same as described in group I.

3.4. Biochemical estimations

At the end of the protocol, animals were euthanized by cervical dislocation and brains were removed carefully. The different parts of the brain i.e. cortex and hippocampus were separated. Isolated parts were homogenized in ice cold phosphate buffer pH 7.4. The homogenate was centrifuged at 14,500 rpm for 15 min at 4 °C. The clear supernatant was used for estimation of thiobarbituric acid reactive substance (TBARS), reduced glutathione (GSH), and brain AChE activity.

3.4.1. Estimation of thiobarbituric acid reactive substance (TBARS)

The TBARS level was estimated in mice brain homogenates, respectively, as an index of lipid peroxidation by the method of Ohkawa, *et al.*²²

3.4.2. Estimation of reduced glutathione (GSH) level

The GSH level was estimated in mice brain homogenates by the method reported by Beutler, *et al.*²³

3.4.3. Estimation of brain AChE activity

The brain AChE activity was measured by following method.¹⁰

4. Statistical analysis

The results were expressed as mean \pm standard deviation. The data obtained from various groups was statistically analyzed by two-way ANOVA followed by Tukey's multiple comparison tests. A value of $p < 0.05$ was considered to be statistically significant.

5. Conclusion

Novel flavonoids based potential polyfunctional agents were synthesized to manage AD. Most of the compounds showed the AChE inhibitory with good radical scavenging and AGEs product formation inhibitory activity. The SAR revealed the influence of varied methoxy groups on ring-B and length of alkyl chain of cyclic amino alkyloxy group on ring-A of flavonoid on AChE inhibition. The compound **7m** ($IC_{50} = 5.87$ nM) was 2-fold more potent than donepezil for AChE inhibition. Moreover, the *in silico* pharmacokinetic profiles revealed that all compounds have drug like properties. The molecular modeling study indicated that compound **7m** simultaneously bind with both PAS and CAS of active site gorge. Additionally, the compound had significant capacity to absorb free radicals and inhibit the AGEs product formation. The compound **7m** also ameliorated scopolamine induced amnesia in mice in terms of restoration of ELT and TSTQ. Thus, the polyfunctional attribute of these flavonoids make them potential candidates for the AD management.

Acknowledgments

I am grateful to my colleagues and assistants for this study and editorial assistance with the manuscript. We wish to thank the 'Indian Council of Medical Research (ICMR)', New Delhi, for providing us a Senior Research Fellowship (ICMR-SRF); Award No. BIC/11(11)/2014. Sophisticated Instrument Centre (SIC), Punjabi University, Patiala, Punjab, India and SAIF, Punjab University, Chandigarh, Punjab, India is acknowledged for providing access to spectrofluorometer and spectral facilities.

Disclosure statement

The authors declare that they have no conflict of interests.

References

- (1) Cardozo MG, Kawai T, Iimura Y, Sugimoto H, Yamanishi Y, Hopfinger A, Sugimoto H, Yamanishi Y, Hopfinger AJ. Conformational analyses and molecular-shape comparisons of a series of indanone-benzylpiperidine inhibitors of acetylcholinesterase. *J Med Chem* 1992;35:590-601.

- (2) Singh M, Kaur M, Chadha N, Silakari O. Hybrids: a new paradigm to treat Alzheimer's disease. *Mol Divers* 2016;20:271-297.
- (3) (a) Bartolini M, Bertucci C, Cavrini V, Andrisano V. β -Amyloid aggregation induced by human acetylcholinesterase: inhibition studies. *Biochem Pharmacol* 2003;65:407-416; (b) Rees T, Hammond PI, Soreq H, Younkin S, Brimijoin S. promotes beta-amyloid plaques in cerebral cortex. *Neurobiol Aging* 2003;24:777-787.
- (4) Singh M, Kaur M, Kukreja H, Chugh R, Silakari O, Singh D. Acetylcholinesterase inhibitors as Alzheimer therapy: from nerve toxins to neuroprotection. *Eur J Med Chem* 2013;70:165-188.
- (5) He Y, Yao PF, Chen SB, Huang ZH, Huang SL, Tan JH, Li D, Gu LQ, Huang ZS. Synthesis and evaluation of 7, 8-dehydrorutaecarpine derivatives as potential multifunctional agents for the treatment of Alzheimer's disease. *Eur J Med Chem* 2013;63:299-312.
- (6) Münch G, Thome J, Foley P, Schinzel R, Riederer P. Advanced glycation end products in ageing and Alzheimer's disease. *Brain Res Rev* 1997;23:134-147.
- (7) (a) Singh M, Kaur M, Silakari O. Flavones: an important scaffold for medicinal chemistry. *Eur J Med Chem* 2014;84:206-239; (b) Solanki I, Parihar P, Mansuri ML, Parihar MS. Flavonoid-based therapies in the early management of neurodegenerative diseases. *Adv Nutr* 2015;6:64-72.
- (8) Singh M, Silakari O. Design, synthesis and biological evaluation of novel 2-phenyl-1-benzopyran-4-one derivatives as potential poly-functional anti-Alzheimer's agents. *RSC Adv* 2016;6:108411-108422.
- (9) (a) Baker W. Molecular rearrangement of some o-acyloxyacetophenones and the mechanism of the production of 3-acylchromones. *J Chem Soc* 1933;10:1381-1389; (b) Mahal HS, Venkataraman K. Synthetical experiments in the chromone group. Part XIV. The action of sodamide on 1-acyloxy-2-acetonaphthones. *J Chem Soc* 1934;56:1767-1769.
- (10) Ellman GL, Courtney KD, Andres V, Featherstone RM. A new and rapid colorimetric determination of acetylcholinesterase activity. *Biochem Pharmacol* 1961;7:88-95.
- (11) Matsuura N, Aradate T, Sasaki C, Kojima H, Ohara M, Hasegawa J, Ubukata M. Screening system for the Maillard reaction inhibitor from natural product extracts. *J Health Sci* 2002;48:520-526.

- (12) Blois MS. Antioxidant determinations by the use of a stable free radical. *Nature* 1958;181:1199-1200.
- (13) Rice-Evans CA, Miller NJ, Paganga G. Structure-antioxidant activity relationships of flavonoids and phenolic acids. *Free Rad Bio Med* 1996;20:933-956.
- (14) Ligprep, version 2.5; Schrodinger, LLC, New York, 2011.
- (15) Kryger G, Silman I, Sussman JL. Structure of acetylcholinesterase complexed with E2020 (Aricept®): implications for the design of new anti-Alzheimer drugs. *Structure* 1999; 7:297-307.
- (16) Glide, version 5.6; Schrodinger, LLC, Newyork, NY, 2010.
- (17) Bowers KJ, Chow E, Xu H, et al. Scalable algorithms for molecular dynamics simulations on commodity clusters, Proceedings of the ACM/IEEE. IEEE, 2006, pp 43.
- (18) QikProp, Version 3.5; Schrödinger, LLC: New York, NY, 2012.
- (19) Lipinski CA, Lombardo F, Dominy BW, Dror RO, Eastwood MP, Gregersen BA, Klepeis JL, Kolossvary I, Moraes MA, Sacerdoti FD, Salmon JK. Experimental and computational approaches to estimate solubility and permeability in drug discovery and development settings. *Adv Drug Deliv Rev* 1997;46:3-26.
- (20) Kelder J, Grootenhuis PD, Bayada DM, Delbressine LP, Ploemen JP. Polar molecular surface as a dominating determinant for oral absorption and brain penetration of drugs. *Pharm Res* 1999;16:1514-1519.
- (21) Morris R. Developments of a water-maze procedure for studying spatial learning in the rat. *J Neurosci Methods* 1984;11:47-60.
- (22) Ohkawa H, Ohishi N, Yagi K. Assay for lipid peroxides in animal tissues by thiobarbituric acid reaction. *Anal Biochem* 1979;95:351-358.
- (23) Beutler E, Duron O, Kelly BM. Improved method for the determination of blood glutathione. *J Lab Clin Med* 1963;61:882-888.

Figures Legends

Fig. 1. Lineweaver–Burk plot from the substrate–velocity curves of the AChE activity with different substrate concentrations (0.05–0.5 mM) in the absence and presence of compound **7m** at 2, 5 and 10 μ M.

Fig. 2. Docked pose of interactions of compound **7m** with AChE active site (1EVE) using Glide. (A) 2D representation of different interactions of **7m** with TcAChE. (B) 3D representation of different interactions of compound **7m** with residues in the binding sites of TcAChE. The compound is rendered in green stick model and the residues are rendered in blue sticks. Hydrogen bonds are indicated with green dashed lines. Residues involved in hydrophobic interactions with the ligand are shown with dashed lines. (C) The TcAChE enzyme is depicted in surface view and compound **7m** as stick in the binding pocket.

Fig. 3. post-MD hydrogen bonds and hydrophobic interactions of **7m** with AChE. (A) Protein interactions fractions with the ligand (**7m**) plot throughout the simulation. (B) protein-ligand contacts plot of compound **7m** with AChE (C) RMSD trajectory plot for compound **7m**.

Fig. 4. Effect different interventions on escape latency time (ELT) at day 1 and day 4 using Morris water maze for memory evaluation. Data was presented as Mean \pm S.D. and analyzed by two way ANOVA followed by Tukey's multiple range test;

^ap < 0.05 vs day 1 ELT in normal; ^bp < 0.05 vs day 4 ELT in normal; ^cp < 0.05 vs day 4 ELT in vehicle + scopolamine; ^dp < 0.05 vs day 4 ELT in donepezil + scopolamine.

Fig. 5. Effect of different interventions on time spent in target quadrant (TSTQ), that is, Q4 in Morris water maze test for memory evaluation. Values are expressed as mean±S.D. and analyzed using two way ANOVA followed by Tukey's multiple range test.

^ap <0.05 versus time spent in other quadrants (Q1, Q2, and Q3) in normal; ^bp <0.05 versus TSTQ in normal; ^cp <0.05 versus TSTQ in vehicle + scopolamine treated; ^dp < 0.05 vs TSTQ in donepezil + scopolamine.

Scheme 1: The synthetic methodology employed to develop compound **5(a-c)**.

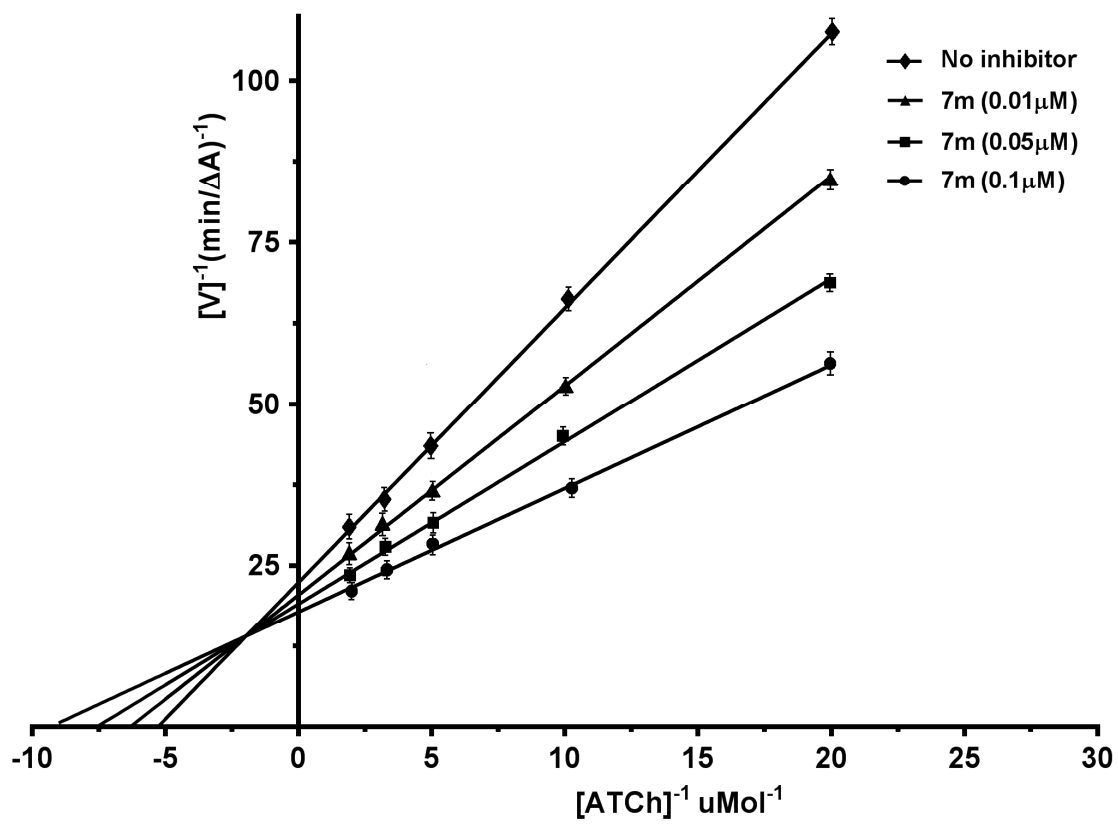
Scheme 2: Synthetic scheme for the synthesis of intermediates **6(a-g)** of flavonoid derivatives

Scheme 3: Synthetic scheme for final compounds **7(a-n)**.

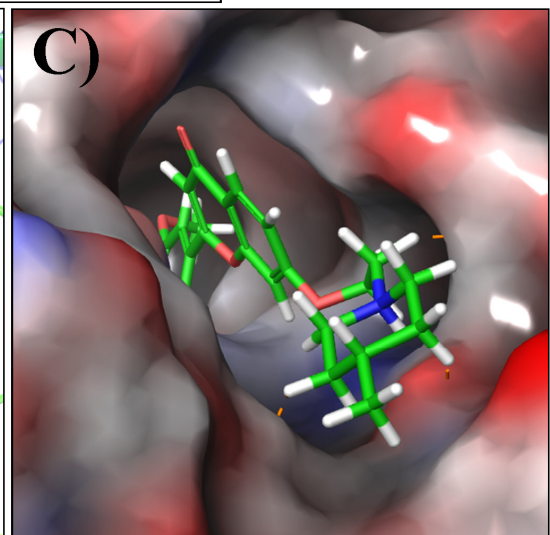
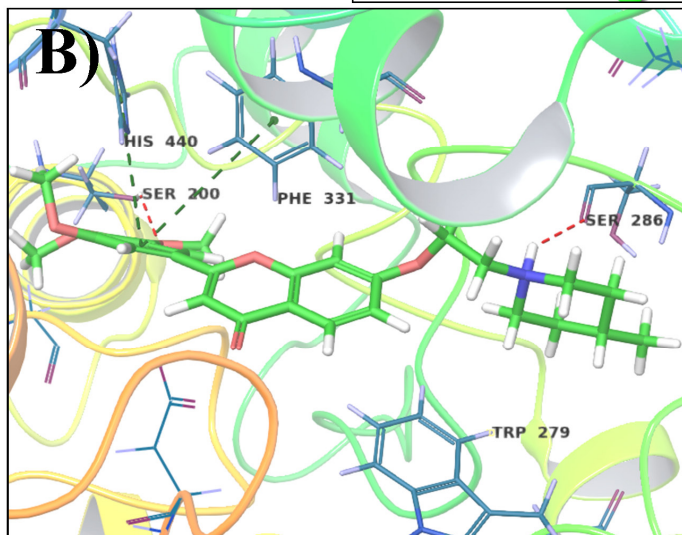
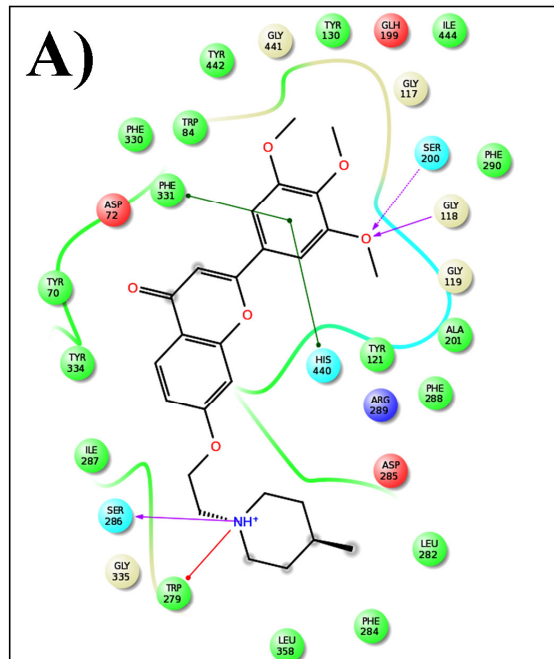
Table 1: The AChE inhibition, Radical scavenging activities and advanced glycation end products (AGEs) formation inhibitory activity of compounds **5(a-c)** and **7(a-n)**.

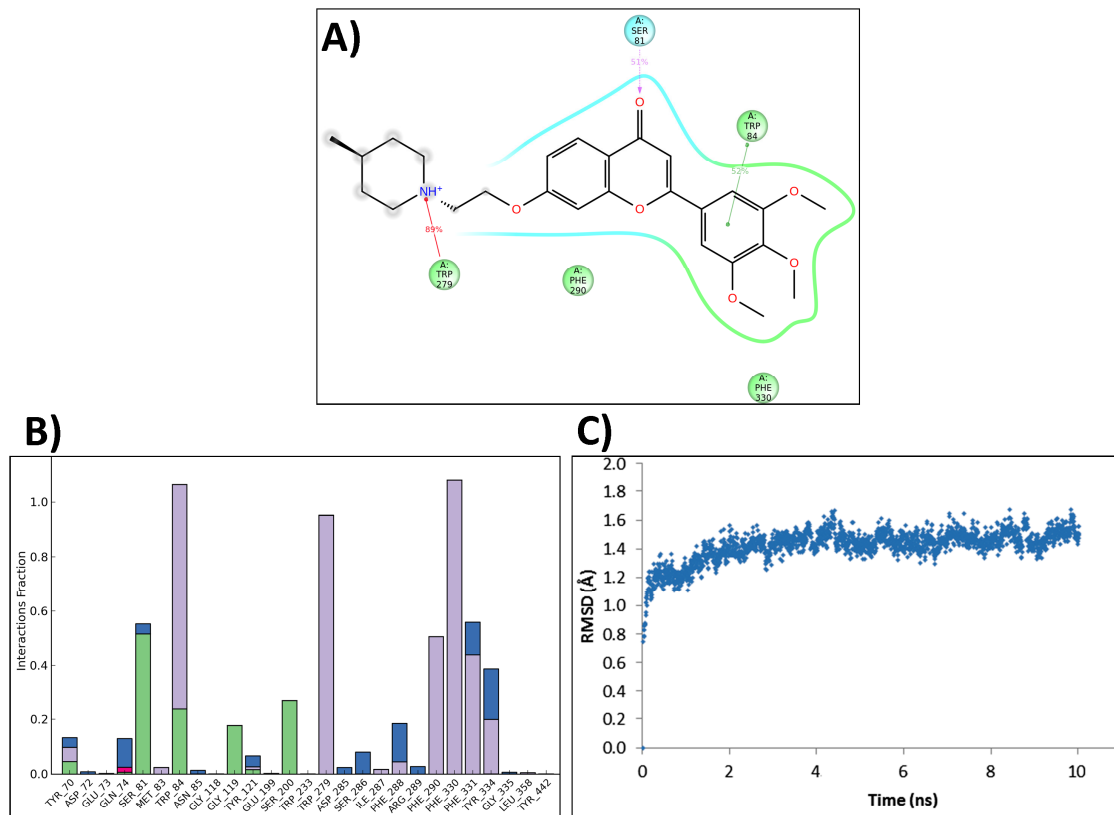
Table 2: Predicted ADMET properties of the target compounds

Table 3: Effect of most active compound **7m**, on AChE activity and oxidative stress (TBARS and GSH) in rat brain.

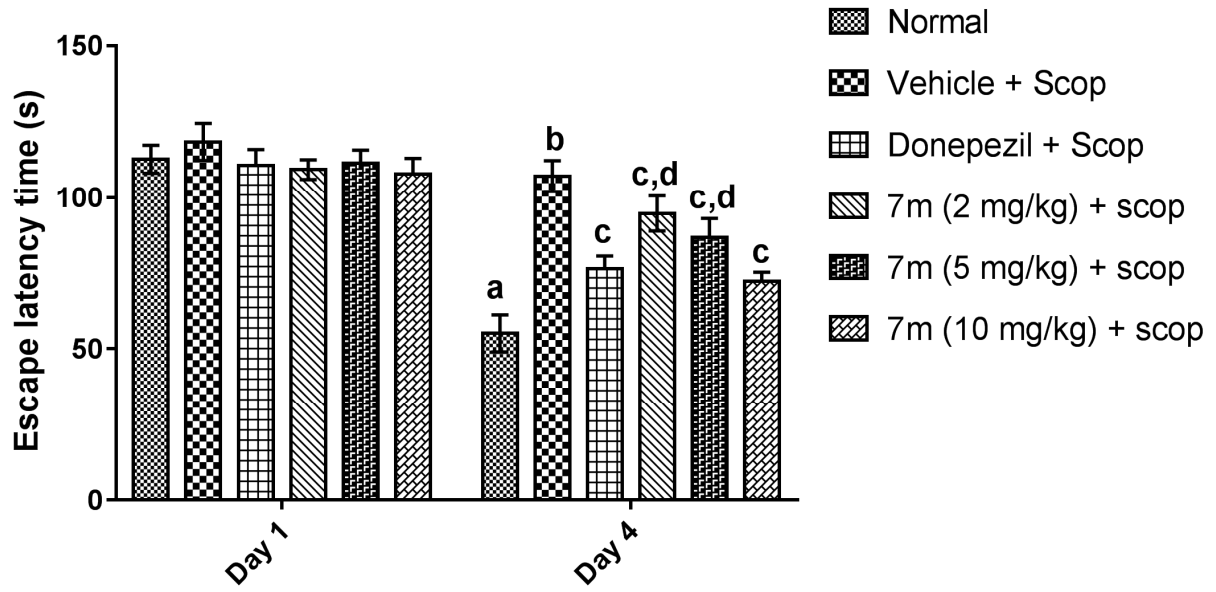


ACCEPTED

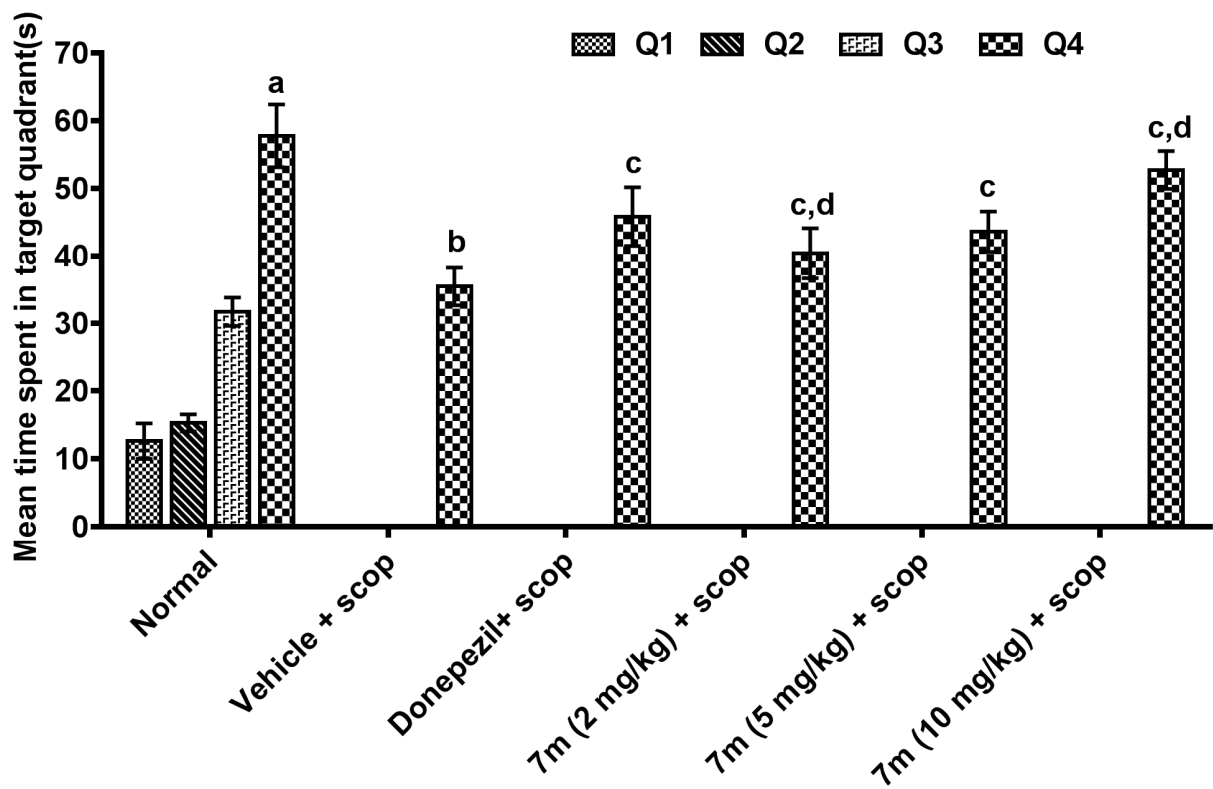


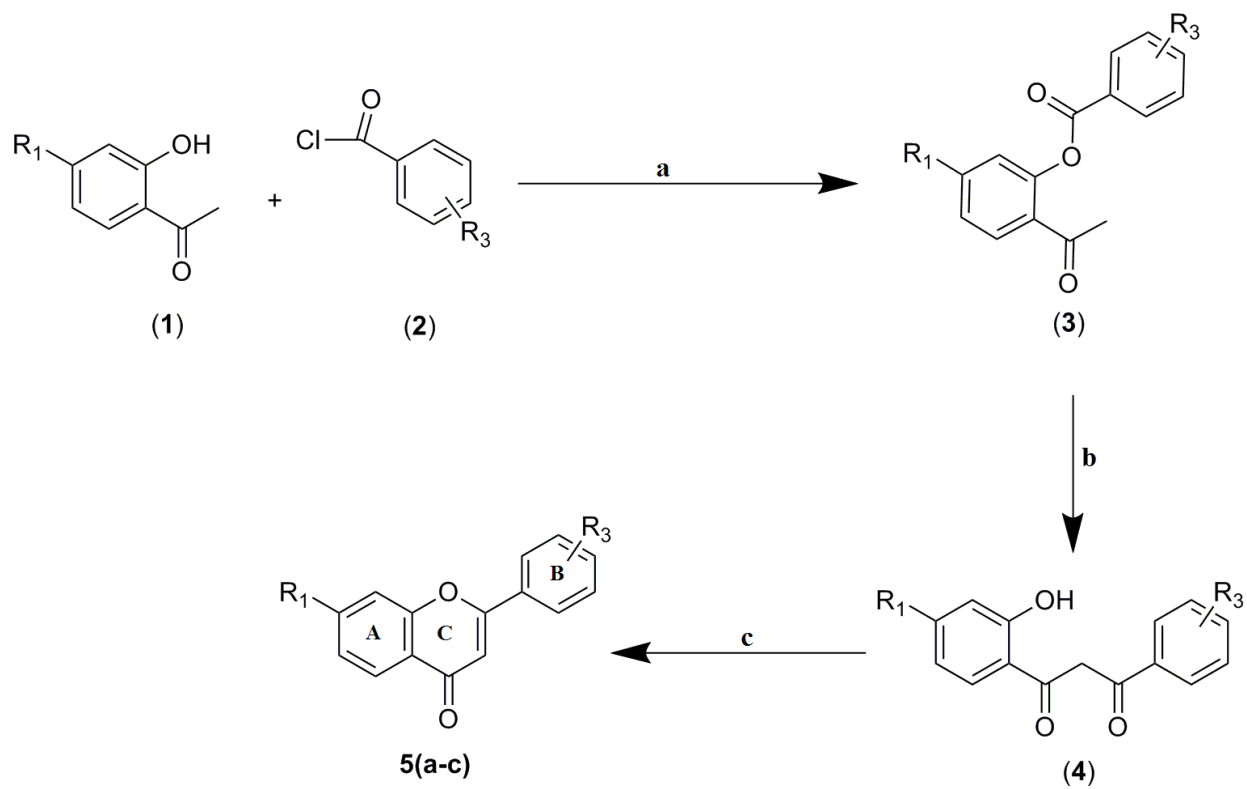


ACCEPTED



ACCEPTED MANUSCRIPT



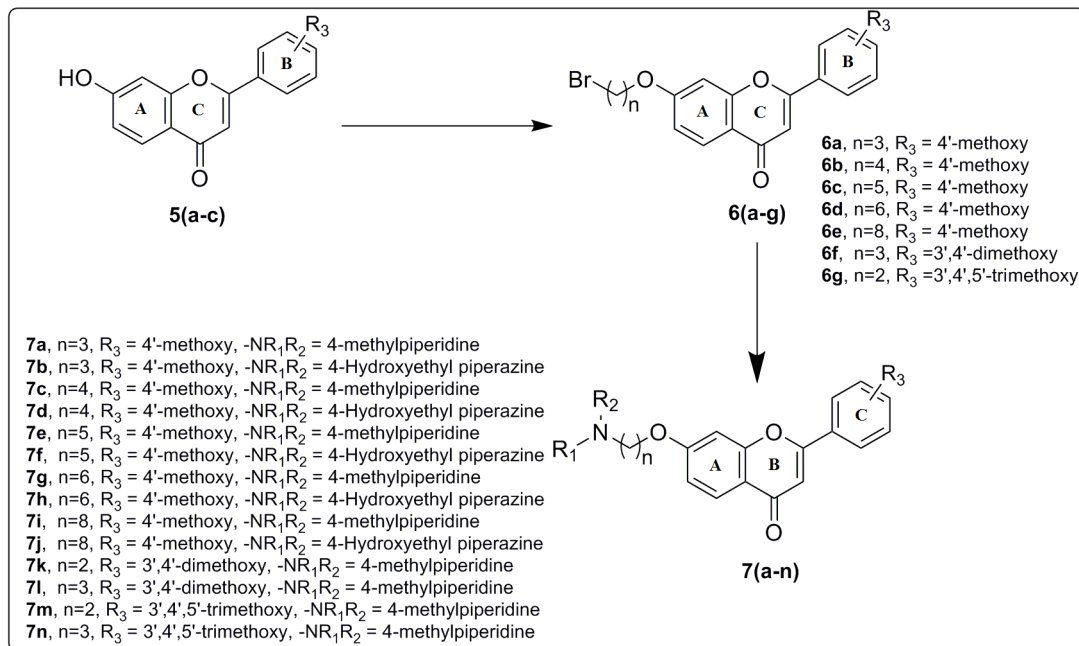


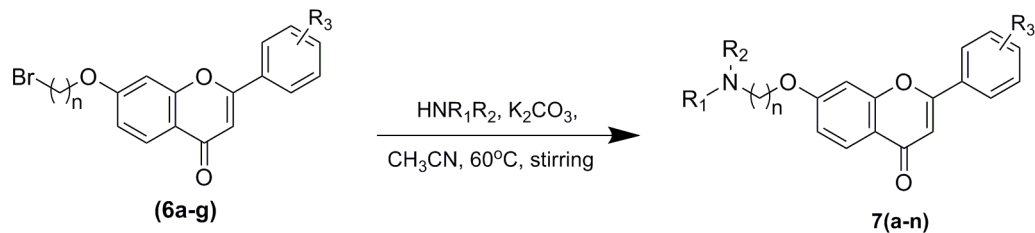
5a = $R_1 = -OH$, $R_3 = 4'$ -methoxy

5b = $R_1 = -OH$, $R_3 = 3',4'$ -dimethoxy

5c = $R_1 = -OH$, $R_3 = 3',4',5'$ -trimethoxy

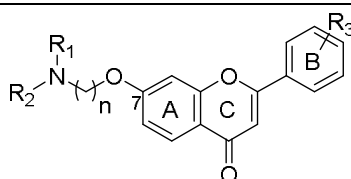
ACCEPTED





- 6a**, n=3, R₃ = 4'-methoxy
6b, n=4, R₃ = 4'-methoxy
6c, n=5, R₃ = 4'-methoxy
6d, n=6, R₃ = 4'-methoxy
6e, n=8, R₃ = 4'-methoxy
6f, n=3, R₃ = 3',4'-dimethoxy
6g, n=2, R₃ = 3',4',5'-trimethoxy

- 7a**, n=3, R₃ = 4'-methoxy, -NR₁R₂ = 4-methylpiperidine
7b, n=3, R₃ = 4'-methoxy, -NR₁R₂ = 4-Hydroxyethyl piperazine
7c, n=4, R₃ = 4'-methoxy, -NR₁R₂ = 4-methylpiperidine
7d, n=4, R₃ = 4'-methoxy, -NR₁R₂ = 4-Hydroxyethyl piperazine
7e, n=5, R₃ = 4'-methoxy, -NR₁R₂ = 4-methylpiperidine
7f, n=5, R₃ = 4'-methoxy, -NR₁R₂ = 4-Hydroxyethyl piperazine
7g, n=6, R₃ = 4'-methoxy, -NR₁R₂ = 4-methylpiperidine
7h, n=6, R₃ = 4'-methoxy, -NR₁R₂ = 4-Hydroxyethyl piperazine
7i, n=8, R₃ = 4'-methoxy, -NR₁R₂ = 4-methylpiperidine
7j, n=8, R₃ = 4'-methoxy, -NR₁R₂ = 4-Hydroxyethyl piperazine
7k, n=2, R₃ = 3',4'-dimethoxy, -NR₁R₂ = 4-methylpiperidine
7l, n=3, R₃ = 3',4'-dimethoxy, -NR₁R₂ = 4-methylpiperidine
7m, n=2, R₃ = 3',4',5'-trimethoxy, -NR₁R₂ = 4-methylpiperidine
7n, n=3, R₃ = 3',4',5'-trimethoxy, -NR₁R₂ = 4-methylpiperidine

Table 1: The AChE inhibition, Radical scavenging activities and advanced glycation end products (AGEs) formation inhibitory activity of compounds **5(a-c)** and **7(a-n)**.

C. No.	-NR ₁ R ₂	n	R ₃	AChE Inhibitory Activity (IC ₅₀ ^b ± SD ^a , nM)	Radical scavenging activity (EC ₅₀ ^c ± SD ^a , nM)	AGEs Inhibitory Activity (IC ₅₀ ^d ± SD ^a , μM)
5a	7-hydroxy	-	4'-methoxy	35.0±0.84	20.5± 0.54	42.0±1.82
5b	7-hydroxy	-	3',4',5'-Trimethoxy	37.3±0.30	22.4±1.01	47.4±0.94
5c	7-hydroxy	-	3',4'-Dimethoxy	44.2±0.30	26.4±1.01	51.4±0.94
7a	4-methylpiperidine	3	4'-methoxy	7.70±1.47	26.58±1.89	42.60±1.85
7b	4-(hydroxyethyl)piperazine	3	4'-methoxy	8.25±0.74	22.78±2.48	43.15±2.19
7c	4-methylpiperidine	4	4'-methoxy	13.53±1.52	28.13±1.86	48.24±1.92
7d	4-(hydroxyethyl)piperazine	4	4'-methoxy	16.50±1.16	23.17±2.02	38.42±1.46
7e	4-methylpiperidine	5	4'-methoxy	15.6 ±1.84	31.7±3.12	55.12±1.08
7f	4-(hydroxyethyl)piperazine	5	4'-methoxy	17.3±2.13	27.9±1.44	49.36±0.85
7g	4-methylpiperidine	6	4'-methoxy	48.12±1.52	32.56±1.49	57.23±0.92
7h	4-(hydroxyethyl)piperazine	6	4'-methoxy	65.7±1.16	34.4±1.25	50.4±1.85
7i	4-methylpiperidine	8	4'-methoxy	57.2 ±1.84	42.6±2.35	61.64±1.75
7j	4-(hydroxyethyl)piperazine	8	4'-methoxy	67.2±2.13	35.7±1.57	52.7±1.84
7k	4-methylpiperidine	2	3',4'-Dimethoxy	6.77±1.18	22.75±1.56	42.1±0.87
7l	4-methylpiperidine	3	3',4'-Dimethoxy	6.48±1.89	24.12±1.84	47.7±1.12
7m	4-methylpiperidine	2	3',4',5'-Trimethoxy	5.87±0.53	23.0±1.47	37.12±0.98
7n	4-methylpiperidine	3	3',4',5'-Trimethoxy	6.12±0.92	26.8±1.80	41.75±1.41
Std.	Donepezil			12.7±0.20	-	
Std.	Ascorbic acid			-	20.0± 0.54	
Std.	Aminoguanidine (AG)			-	-	40.06±1.78

^aSD: Data are expressed as mean ± SD (n=3). Data were statistically analyzed by one way ANOVA; *P<0.05 vs Std.

^bIC₅₀, inhibitor concentration (means ± SD of three experiments) for 50% inactivation of AChE.

^cEC₅₀ was defined as the effective concentration resulting in 50% scavenging activity.

^dIC₅₀ was defined as the concentration resulting in 50% inhibition of AGEs product formation.

Table 2: Predicted ADMET properties of the target compounds

Comp.	Mol_MW ^a (130-725)	HB donors ^a (0-6)	HB acceptors ^a (2-20)	QIPo/w ^a (-2 to 6.5)	PSA ^a (7-200)	SASA ^a (300-1000)	Rule of Five	CNS ^a	QPPM DCK (<25poor, >500great)	QPP Caco ^a (<25poor, >500great)	QIPogB ^a (-3 to 1.2)	QIPogKhsa ^a (-1.5 to 1.5)	QIPlogS ^a (-6.5 to 0.5)	% Human Oral Absorption ^a (>80% high, <25% poor)	Calculated MMGBSA Binding Energy (kcal/mol) AChE
5a	256.233	1	3.25	2.732	57.902	480.146	0	0	804.318	905.688	0.357	0.126	3.931	95.864	-42.534
5b	328.321	1	5.5	2.794	77.547	578.238	0	-1	444.396	905.536	0.713	0.127	4.145	96.229	-66.75
5c	298.295	1	4.75	2.748	71.089	552.813	0	0	444.415	905.572	0.654	0.136	4.175	95.962	57.588
7a	407.508	0	6	4.779	56.335	782.371	0	1	386.830	725.384	0.039	0.754	5.705	100	87.035
7b	438.522	1	9.7	2.688	85.038	817.997	0	1	238.284	649.072	0.539	0.156	3.519	72.945	97.835
7c	421.535	0	6	5.172	56.337	815.061	1	1	386.889	725.486	0.115	0.887	6.162	95.473	78.268
7d	452.549	1	9.7	3.061	85.04	850.701	0	1	382.287	629.079	0.632	0.269	-3.93	75.134	99.832
7e	435.562	0	6	5.568	56.336	848.139	1	1	386.994	725.669	0.192	1.02	6.426	100	74.188
7f	466.576	1	9.7	3.438	85.039	883.775	0	0	207.294	679.091	0.725	0.384	4.352	77.343	95.992
7g	449.589	0	6	5.964	56.338	881.149	1	1	386.961	725.612	0.268	1.154	7.089	100	62.498
7h	480.603	1	9.7	3.816	85.041	916.776	0	0	231.292	769.088	0.818	0.5	4.775	79.554	88.721
7i	477.642	0	6	6.754	56.337	947.050	1	1	386.975	725.635	-0.42	1.42	6.012	100	74.475
7j	508.656	1	9.7	4.57	85.0	982.	1	-2	213.29	749.0	-	0.7	-	71.04	-

				5	42	771			3	89	1.00 2	36	5.62 9	1	98.33 7
7k	423.5 08	0	6.7 5	4.49 2	59.4 82	786. 990	0	1	382.98 3	718.7 08	0.03 9	0.6 14	-5.4	100	75.26 7
7l	437.5 35	0	6.7 5	4.91 5	61.3 07	825. 338	0	1	384.22 6	720.8 66	0.12 1	0.7 56	5.96 4	100	81.99 5
7m	453.5 34	0	7.5	4.51 8	65.9 26	812. 684	0	1	382.93 4	718.6 23	-0.1	0.5 66	5.33 1	100	87.89 7
7n	467.5 61	0	7.5	4.94 7	67.6 42	852. 640	0	1	386.78 8	725.3 11	0.18 1	0.7 09	5.92 6	100	84.69 1
Std.	379.4 98	0	5.5	4.46 7	44.6 12	723. 535	0	1	501.72 0	922.6 94	0.11 8	0.6 21	- 4.85 2	100	-78.70

^aMW: molecular weight, HBD: hydrogen-bond donor atoms, HBA: hydrogen-bond acceptor atoms, QPlogPo/w: Predicted octanol/water partition coefficient, PSA: polar surface area, SASA: total solvent accessible surface area, CNS: Predicted central nervous system activity on a -2 (inactive) to +2 (active) scale, QPPMDCK: Predicted apparent MDCK cell permeability in nm/sec, QPPCaco: Caco-2 cell permeability in nm/sec, QPlogBB: brain/blood partition coefficient, QPlogKhsa: binding to human serum albumin, QPlogS: Predicted aqueous solubility, Percent Human-Oral Absorption: human oral absorption on 0 to 100% scale, Std.= Donepezil.

Table 3: Effect of most active compound **7m**, on AChE activity and oxidative stress (TBARS and GSH) in rat brain.

Compound	TBARS (nM/mg)	GSH (nM/mg)	AChE activity (nM/min/mg protein)
Normal	15.52±0.98	39.7±0.78	0.71±0.02
Vehicle + scop	26.51±0.79 ^a	21.3±0.81 ^a	1.25±0.04 ^a
Donepezil + scop	18.13±0.81 ^b	34.6±0.74 ^b	0.82±0.05 ^b
7m (2 mg/kg) + scop	24.27±0.67 ^{b,c}	24.1±1.10 ^{b,c}	1.07±0.06 ^{b,c}
7m (5 mg/kg) + scop	20.14±0.97 ^{b,c}	31.7±0.63 ^{b,c}	0.97±0.02 ^{b,c}
7m (10 mg/kg) + scop	17.6±0.42 ^b	36.8±1.25 ^{b,c}	0.85±0.03 ^b

Data are presented as mean±standard deviation; analysed by one way ANOVA followed by Tukey's multiple comparison test.

^aSignificant difference ($p < 0.05$) in comparison to normal.

^bSignificant difference ($p < 0.05$) in comparison to Vehicle + scop.

^cSignificant difference ($p < 0.05$) in comparison to Donepezil + scop.

Graphical Abstract

Exploration of chromen-4-one based scaffold's potential in Alzheimer's disease: Design, Synthesis and Biological evaluations

Manjinder Singh^a, Maninder Kaur^a, Nirmal Singh^a, Om Silakari^{a,*}

ABSTRACT:

A novel series of flavonoid based compounds were designed, synthesized and biologically evaluated for Acetylcholinesterase (AChE) inhibitory activity integrated with advanced glycation end products (AGEs) inhibitory and antioxidant potential. Most of the derivatives inhibited AChE in nanomolar IC₅₀ range along with good AGEs inhibitory and radical scavenging activity. Thus, flavonoids might be the promising lead compounds as potential polyfunctional anti-Alzheimer's agents.

